Z strain of SeV did not affect resistance to HIV-1-GFP infection. For negative control, we used another recombinant SeV expressing AGM-TRIM5α-CC(−)-HA. Expression of this mutant TRIM5α was at a level similar to that of the wild type TRIM5α in MT-4 cells (Fig. 1C). As expected, cells infected with SeV expressing AGM-TRIM5α-CC(−) were also resistant to HIV-1-GFP infection. In contrast, cells infected with SeV expressing HA-AGM-TRIM5γ showed greatly increased sensitivity to HIV-1 infection. Cells infected with SeV expressing CM-TRIM5α-SPRY(−) also became sensitive to HIV-1 infection, while the level of the dominant-negative effect of CM-TRIM5α-SPRY(−) was similar to that of AGM TRIM5γ.

3.2. Dominant-negative effect of truncated mutant of TRIM5α or of TRIM5γ on TRIM5α of different primate species

TRIM5 variants lacking the SPRY domain were then examined whether they have a dominant-negative effect on TRIM5α of different primate species. As shown in Fig. 2, HIV-1 infection was severely restricted by CM, Rh, and AGM TRIM5αs and Hu TRIM5α with R332P (Yap et al., 2005), while HIV-1 replicated in the presence of those same primate TRIM5αs when CM-TRIM5α-SPRY(−) was expressed simultaneously. In contrast, dominant-negative effect of TRIM5γ was relatively weak in this experiment probably due to its lower expression levels (Fig. 1C). These results demonstrate that CM-TRIM5α-SPRY(−) exerts a strong dominant-negative activity on TRIM5α function from various primate species.

3.3. Comparison of silencing effect by siRNA and truncated mutant of TRIM5α or TRIM5γ

The silencing effect of CM-TRIM5α-SPRY(−) or AGM TRIM5γ was compared with that of siRNA on AGM TRIM5 (si-TRIM5). CV1 cells were transfected with si-TRIM5 and the expression levels of TRIM5α was monitored by real-time PCR (Nakayama et al., 2005). TRIM5 mRNA expression levels in the si-TRIM5 transfected CV1 cells were reduced to approximately 25% of those in CV1 cells transfected with control siRNA (Si-Cont) (Fig. 3A), indicating a quite efficient knockdown of endogenous TRIM5α by siRNA. CV1 cells transfected with Si-Cont or si-TRIM5, or those infected with SeV expressing AGM-TRIM5α-CC(−), CM-TRIM5α-SPRY(−), or AGM TRIM5γ, were superinfected with HIV-1-GFP and the infected cells were counted after 48 h. HIV-1-GFP infection in si-TRIM5 transfected cells was enhanced 3–10-fold (depending on the viral dose) compared with that in Si-Cont-transfected cells (Fig. 3B). In cells expressing CM-TRIM5α-SPRY(−), HIV-1-GFP infection was enhanced 8–30 times (depending on the viral dose) more than in cells expressing AGM-TRIM5α-CC(−) (Fig. 3B). AGM TRIM5γ showed similar effect to CM-TRIM5α-SPRY(−). Compared with cells transfected with si-TRIM5, those infected with SeV expressing CM-TRIM5α-SPRY(−) or AGM TRIM5γ were rendered more vulnerable to infection by HIV-1-GFP (2.7–3.0-fold). In addition, CV1 cells transfected with si-TRIM5 and subsequently infected with SeV expressing CM-TRIM5α-SPRY(−) or AGM TRIM5γ were more infected with HIV-1-GFP than those with si-TRIM5 alone. These results suggest that the silencing effect of TRIM5 variants lacking SPRY domain is much more efficient than that of si-TRIM5.

3.4. Exogenous expression of TRIM5α, TRIM5γ, or truncated mutant of TRIM5α did not affect an entry step of HIV-1 infection

To exclude a possibility that exogenous AGM TRIM5γ or CM TRIM5α lacking the SPRY domain could not interfere with endogenous TRIM5α but could enhance an entry step HIV-1, a gene reported cell fusion assay was performed. CV1 cells expressing various TRIM5s, human CD4, and human CXCR4 were prepared, and those cells were mixed with mouse L cells expressing HIV-1 envelope protein. As shown in Fig. 4, cells expressing TRIM5α were equally sensitive to the envelope-mediated cell fusion to those expressing TRIM5γ or truncated mutants of TRIM5α. These results clearly indicated that TRIM5γ and truncated mutant of TRIM5α did not enhance viral entry.

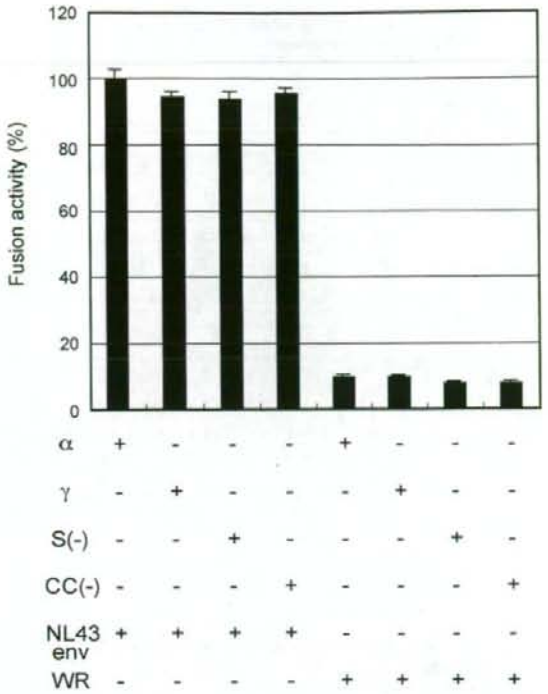

Fig. 4. Exogenous expression of TRIM5α, TRIM5γ, or truncated mutant of TRIM5α did not affect an entry step of HIV-1 infection. Mouse L cells were transfected with β-galactosidase reporter plasmid and infected with a recombinant Vac expressing NL43 envelope (env) or parental WR strain. At the same time, CV1 cells were infected with SeV expressing human CXCR4 and AGM TRIM5α (α), AGM TRIM5γ (γ), CM-TRIM5α-SPRY(−) (S(−)), or AGM-TRIM5α-coiled-coil(−) (CC(−)) and with Vacs expressing T7 RNA polymerase and human CD4. Then, L and CV1 cells were mixed, and β-galactosidase activities in the cell lysate were measured. The representative results of two independent experiments with similar results are shown. Error bars denote S.D. of triplicate samples.

3.5. Colocalization of truncated mutant of TRIM5α or TRIM5γ with TRIM5α

A confocal microscope was used to examine the subcellular localization of truncated mutant of TRIM5α or TRIM5γ. As shown in Fig. 5A, AGM TRIM5α formed cytoplasmic bodies but also exhibited diffuse cytoplasmic staining, thus confirming previous findings (Javanbakht et al., 2005). Compared with AGM TRIM5α, TRIM5γ tended to locate around the nuclear membrane to form more but smaller cytoplasmic bodies. In contrast, CM TRIM5α lacking the SPRY domain formed much larger cytoplasmic bodies than those of AGM TRIM5α, although the composition of CM TRIM5α lacking the SPRY domain resembled that of TRIM5γ. AGM TRIM5α lacking the SPRY domain [AGM-TRIM5α-SPRY(−)-HA] showed a similar subcellular localization to CM TRIM5α lacking the SPRY domain.

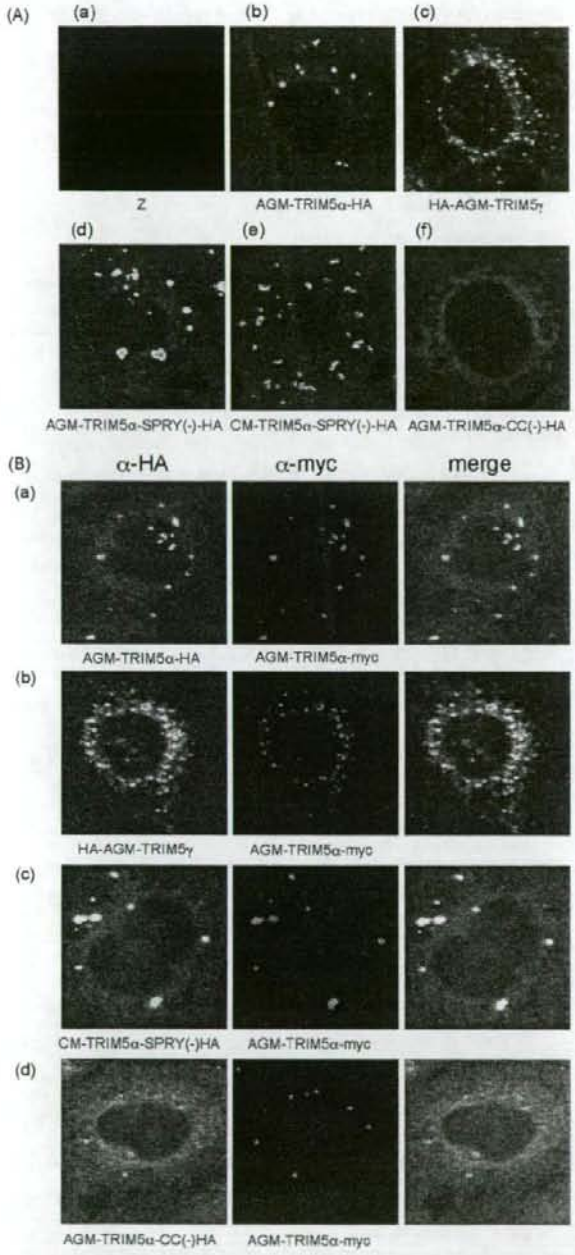

Fig. 5. (A) Subcellular localization of TRIM5s. CV1 cells infected with SeV expressing HA-tagged TRIM5 proteins at MOI of 10 PFU per cell were analyzed as described in Section 2. Representative confocal microscopic images are shown of the CV1 cells infected with parental Z strain of SeV (a), or with SeV expressing AGM TRIM5α (b), AGM TRIM5γ (c), AGM-TRIM5α-SPRY(−) (d), CM-TRIM5α-SPRY(−) (e), or AGM-TRIM5α-CC(−) (f). (B) Colocalization of HA-tagged TRIM5 variants and myc-tagged AGM TRIM5α. CV1 cells infected with SeV expressing HA-tagged TRIM5 and myc-tagged TRIM5α at MOI of 5 PFU per cell were analyzed as described in Section 2. Representative confocal microscopic images of the CV1 cells infected with SeV expressing TRIM5α-myc and SeV expressing one of the following proteins: AGM-TRIM5α-HA (a), HA-AGM-TRIM5γ (b), CM-TRIM5α-SPRY(−)-HA (c), or AGM-TRIM5α-CC(−)-HA (d). The overlay of *green* and *red* fluorescence is shown in the *right panels*.

Thus, the unique subcellular localization of TRIM5γ is due to the specific sequence of TRIM5γ and disruption of the SPRY domain causes significant changes in the subcellular localization of TRIM5α. In contrast, AGM-TRIM5α-CC(−)-HA showed diffuse cytoplasmic localization (Fig. 5A).

The subcellular localization of various TRIM5s was then examined in the presence of the wild type TRIM5α. In Fig. 5B, HA-tagged and myc-tagged proteins are shown in green (*left panels*) and red (*middle panels*), respectively. The *right panels* represent overlays of the left and middle panels. As expected, AGM-TRIM5α-HA and AGM-TRIM5α-myc colocalized in the cytoplasm (Fig. 5Ba). In cells coexpressing HA-AGM-TRIM5γ and AGM-TRIM5α-myc, both proteins exhibited minor cytoplasmic body staining around the nucleus, similar to the cytoplasmic bodies formed by HA-AGM-TRIM5γ alone (Fig. 5Bb). This result indicates that the coexpression of AGM TRIM5γ causes relocalization of AGM-TRIM5α. Colocalization of CM-TRIM5α-SPRY(−)-HA and AGM-TRIM5α-myc was observed mainly in large cytoplasmic bodies characteristic of CM-TRIM5α-SPRY(−)-HA (Fig. 5Bc). In cells coexpressing AGM-TRIM5α-CC(−)-HA and AGM-TRIM5α-myc, the former displayed diffuse cytoplasmic staining (Fig. 5Bd), while the latter formed cytoplasmic bodies. These results confirm the involvement of the coiled-coil domain in formation of the TRIM5 oligomer.

3.6. Hetero-oligomerization of truncated mutant of TRIM5α or TRIM5γ and TRIM5α

TRIM5α reportedly forms homo-trimers via the coiled-coil domain (Mische et al., 2005). To test whether truncated mutant of TRIM5α or TRIM5γ can form hetero-oligomers with TRIM5α, various HA-tagged TRIM5s and AGM-TRIM5α-myc were subjected to co-immunoprecipitation analysis. Fig. 6 shows the association of AGM-TRIM5α-HA, HA-AGM-TRIM5γ, and CM-TRIM5α-SPRY(−)-

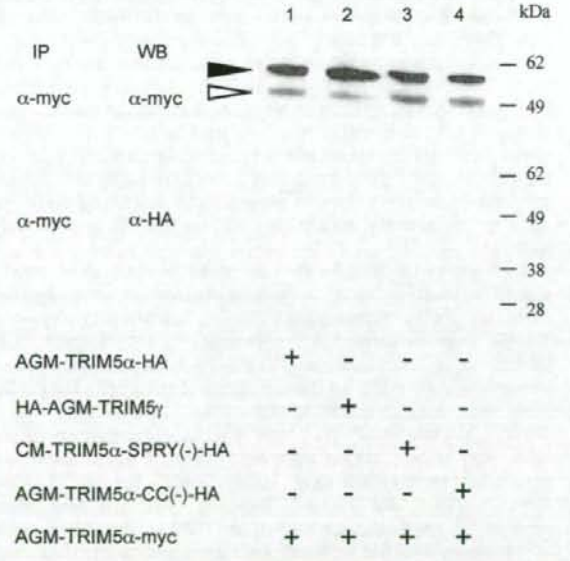

Fig. 6. Co-precipitation analysis of TRIM5 oligomerization. CV1 cells were infected with SeV expressing HA-tagged TRIM5 and myc-tagged AGM TRIM5α at MOI of 5 PFU per cell. After 22 h, the cells were lysed and subjected to immunoprecipitation with an anti-myc antibody. Immunoprecipitates were analyzed by Western blot using the antibodies indicated. Black triangles denote AGM-TRIM5α-myc proteins and white triangles non-specifically reacted proteins.

HA with AGM-TRIM5α-myc. In contrast, AGM-TRIM5α-CC(−)-HA did not show any association with AGM-TRIM5α-myc, confirming involvement of the coiled-coil domain in the self-association of TRIM5α. These results suggest that the dominant-negative effect of CM-TRIM5α-SPRY(−) or AGM TRIM5γ was due to hetero-oligomer formation that prevented binding to the target viral capsid.

4. Discussion

The application of a dominant-negative effect of truncated mutant of TRIM5α to efficient silencing of TRIM5α function without siRNA was demonstrated. Firstly, it was shown that CM TRIM5α lacking the SPRY domain had a dominant-negative effect on AGM, Rh, CM, or Hu-R332P TRIM5α mediated anti-HIV-1 activity. These results suggest that this dominant-negative effect is exerted regardless of TRIM5α primate species. Next the knockdown effect of siRNA was compared with that of TRIM5 variants lacking SPRY domain and it was found that the silencing effect of TRIM5α mediated anti-HIV-1 activity by expression of TRIM5 variants lacking SPRY domain was superior to that of si-TRIM5.

The knockdown effect of siRNA depends on target sequence and transfection efficiency. It was shown previously that HIV-1-GFP infections in Rh cells transduced with vector expressing TRIM5γ is lower than that of Rh cells transfected with the siRNA directed against Rh TRIM5α (Stremlau et al., 2004). The difference between the result of this previous study and the present study was probably due to different expression levels of TRIM5γ. Target of the most efficient siRNA against TRIM5 were coiled-coil region in the previous study (Stremlau et al., 2004), and siRNA was also used against TRIM5α including coiled-coil region in the present study. The difference between the nucleotide sequence of AGM TRIM5α and that of CM or human is 5.9% and 10.8%, respectively, while the difference between the amino acid sequence in the coiled-coil region of AGM TRIM5α and that of CM or human is 5.9% and 9.8%, respectively. This suggests that siRNA-targeting AGM TRIM5 may not be able to knockdown TRIM5α of other primates. Compared with siRNA, the advantage of silencing by TRIM5 variants lacking the SPRY domain is that target sequence and transfection efficiency do not have to be taken into account. A retroviral gene-silencing system was developed for efficient delivery of siRNA, but it takes several weeks to establish such cell lines. For the TRIM5α study, generating only 1 SeV expressing TRIM5 variant lacking the SPRY domain proved to be quick and sufficient for silencing antiviral activity of TRIM5αs from various primate species.

Compared with TRIM5α, the subcellular localization of TRIM5γ tended to locate around the nuclear membrane while forming more but smaller cytoplasmic bodies. It has been reported that TRIM5α proteins forms trimers, whereas TRIM5γ forms dimers (Mische et al., 2005). The size of the cytoplasmic body may be affected by differences in the formation of homo-oligomers. The subcellular localization of TRIM5γ was also different from that of CM or AGM-TRIM5α-SPRY(−). Hydrophobic homopolymeric amino acids such as polyleucine have been found to aggregate in the perinuclear region (Oma et al., 2004). TRIM5γ-specific 33 amino acids contain 9 Leu, 1 Ile, 2 Phe, and 1 Val. It is thus possible that the hydrophobic nature of the TRIM5γ-specific sequence affects its subcellular localization and cytoplasmic body formation.

Many restriction factors have been identified in mammalian cells (Goff, 2004), and new information on these restriction factors may lead the development of new anti-HIV-1 strategies. Identification or characterization of new restriction factors in the absence of TRIM5α-mediated resistance can be expected to clarify the roles of other antiviral proteins. In this study, we were able to demonstrate that TRIM5 variants lacking the SPRY domain expressed by SeV showed a stronger silencing effect on TRIM5α than that expressed by siRNA regardless of primate species. It is considered that this observation can be used for studying restriction factors other than TRIM5α in a variety of mammalian cells.

Acknowledgements

We thank J. Sakuragi and S. Sakuragi for helpful discussions and S. Bando and N. Teramoto for assistance. This work was supported by grants from the Ministry of Education, Culture, Sports, Science, and Technology and the Ministry oh Health, Labor and Welfare, Japan.

References

Adachi, A., Gendelman, H.E., Koeing, S., Folks, T., Willey, R., Rabson, A., Martin, M.A., 1986. Production of acquired immunodeficiency syndrome associated retrovirus in human and nonhuman cells transfected with an infectious molecular clone. J. Virol. 59, 284–291.
Goff, S.P., 2004. Retrovirus restriction factors. Mol. Cell 16, 849–859.
Himathongkham, S., Luciw, P.A., 1996. Restriction of HIV-1 (subtype B) replication at the entry step in rhesus macaque cells. Virology 219, 485–488.
Hofmann, W., Schubert, D., LaBonte, J., Munson, L., Gibson, S., Scammell, J., Ferrigno, P., Sodroski, J., 1999. Species-specific, postentry barriers to primate immunodeficiency virus infection. J. Virol. 73, 10020–10028.
Javanbakht, H., Diaz-Griffero, F., Stremlau, M., Si, Z., Sodroski, J., 2005. The contribution of RING and B-box 2 domains to retroviral restriction mediated by monkey TRIM5α. J. Biol. Chem. 280, 26933–26940.
Kono, K., Song, H., Shingai, Y., Shioda, T., Nakayama, E.E., 2008. Comparison of antiviral activity of rhesus monkey and cynomolgus monkey TRIM5αs against HIV-2 infection. Virology 373, 447–456.
Mische, C.C., Javanbakth, H., Song, B., Diaz-Griffero, F., Stremlau, M., Strack, B., Si, Z., Sodroski, J., 2005. Retroviral restriction factor TRIM5<alpha>is a trimer. J. Virol. 79, 14446–14450.
Miyoshi, H., Takahashi, M., Gage, F.H., Verma, I.M., 1997. Stable and efficient gene transfer into the retina using an HIV-based lentiviral vector. Proc. Natl. Acad. Sci. U.S.A. 94, 10319–10323.
Miyoshi, H., Blomer, U., Takahashi, M., Gage, F.H., Verma, I.M., 1998. Development of a self-inactivating lentivirus vector. J. Virol. 72, 8150–8157.
Nakayama, E.E., Tanaka, Y., Nagai, Y., Iwamoto, A., Shioda, T., 2004. A CCR2-V641 polymorphism affects stability of CCR2A isoform. AIDS 18, 729–738.
Nakayama, E.E., Miyoshi, H., Nagai, Y., Shioda, T., 2005. A specific region of 37 amino acid residues in the SPRY (B30.2) domain of African green monkey TRIM5α determines species-specific restriction of simian immunodeficiency virus SIVmac infection. J. Virol. 79, 8870–8877.
Nakayama, E.E., Maegawa, H., Shioda, T., 2006. A dominant-negative effect of cynomolgus monkey tripartite motif protein TRIM5α on anti-simian immunodeficiency virus SIVmac activity of an African green monkey orthologue. Virology 350, 158–163.
Nussbaum, O., Broder, C.C., Berger, E.A., 1994. Fusogenic mechanism of envelope-virus glycoproteins analyzed by a novel recombinant vaccinia virus-based assay quantitating cell fusion-dependent reporter gene activation. J. Virol. 68, 5411–5422.
Oma, Y., Kino, Y., Sasagawa, N., Ishiura, S., 2004. Intracellular localization of homopolymeric amino acid-containing proteins expressed in mammalian cells. J. Biol. Chem. 279, 21217–21222.
Perez-Caballero, D., Hatziioannou, T., Yang, A., Cowan, S., Bieniarz, P.D., 2005. Human tripartite motif 5α domains responsible for retrovirus restriction activity and specificity. J. Virol. 79, 8969–8978.
Reymond, A., Meroni, G., Fantozzi, A., Merla, G., Cairo, S., Luzi, L., Riganelli, D., Zanaria, E., Messali, S., Cainarca, S., Guffanti, A., Minucci, S., Pelicci, P.G., Ballabio, A., 2001. The tripartite motif family identifies cell compartments. EMBO J. 20, 2140–2151.
Sawyer, S.L., Wu, L.I., Emerman, M., Malik, H.S., 2005. Positive selection of primate TRIM5α identifies a critical species-specific retroviral restriction domain. Proc. Natl. Acad. Sci. U.S.A. 102, 2832–2837.
Sebastian, S., Luban, J., 2005. TRIM5alpha selectively binds a restriction-sensitive retroviral capsid. Retrovirology 2, 40.
Shibata, R., Sakai, H., Kawamura, M., Tokunaga, K., Adachi, A., 1995. Early replication block of human immunodeficiency virus type 1 in monkey cells. J. Gen. Virol. 76, 2723–2730.
Shioda, T., Nakayama, E.E., Tanaka, Y., Xin, X., Liu, H., Kawana-Tachikawa, A., Kato, A., Sakai, Y., Nagai, Y., Iwamoto, A., 2001. Naturally occurring deletional mutation in the C-terminal cytoplasmic tail of CCR5 affects surface trafficking of CCR5. J. Virol. 75, 3462–3468.

Song, B., Javanbakht, H., Perron, M., Park, D.H., Stremlau, M., Sodroski, J., 2005. Retrovirus restriction by TRIM5α variants from Old World and New World Primates. J. Virol. 79, 3930–3937.

Song, H., Nakayama, E.E., Yokoyama, M., Sato, H., Levy, J.A., Shioda, T., 2007. A single amino acid of the human immunodeficiency virus type 2 capsid affects its replication in the presence of cynomolgus monkey and human TRIM5αs. J. Virol. 81, 7280–7285.

Stremlau, M., Owens, C.M., Perron, M.J., Kiessling, M., Autissier, P., Sodroski, J., 2004. The cytoplasmic body component TRIM5α restricts HIV-1 infection in Old World monkeys. Nature 427, 848–853.

Stremlau, M., Perron, M., Welikala, S., Sodroski, J., 2005. Species-specific variation in the B30.2 (SPRY) domain of TRIM5α determines the potency of human immunodeficiency virus restriction. J. Virol. 79, 3139–3145.

Stremlau, M., Perron, M., Lee, M., Li, Y., Song, B., Javanbakht, H., Diaz-Griffero, F., Anderson, D.J., Sundquist, W.I., Sodroski, J., 2006. Specific recognition and accelerated uncoating of retroviral capsids by the TRIM5α restriction factor. Proc. Natl. Acad. Sci. U.S.A. 103, 5514–5519.

Yap, M.W., Nisole, S., Stoye, J.P., 2005. A single amino acid change in the SPRY domain of human Trim5alpha leads to HIV-1 restriction. Curr. Biol. 15, 73–78.

Journal of General Virology (2008), 89, 554–566 DOI 10.1099/vir.0.83186-0

Impact of glycosylation on antigenicity of simian immunodeficiency virus SIV239: induction of rapid V1/V2-specific non-neutralizing antibody and delayed neutralizing antibody following infection with an attenuated deglycosylated mutant

Chie Sugimoto,[1,2,3] Emi E. Nakayama,[4] Tatsuo Shioda,[4] Francois Villinger,[5] Aftab A. Ansari,[5] Naoki Yamamoto,[1] Yasuo Suzuki,[3,6] Yoshiyuki Nagai[7] and Kazuyasu Mori[1,2,3]

Correspondence
Kazuyasu Mori
mori@nih.go.jp

[1]AIDS Research Center, National Institute of Infectious Diseases, Shinjuku-ku, Tokyo 162-8640, Japan

[2]Tsukuba Primate Research Center, National Institute of Biomedical Innovation, Tsukuba, Ibaraki 305-0843, Japan

[3]CREST, Japan Science and Technology Agency, Kawaguchi, Saitama 332-0012, Japan

[4]Department of Viral Infections, Research Institute for Microbial Diseases, Osaka University, Suita, Osaka 565-0871, Japan

[5]Department of Pathology and Laboratory Medicine, Emory University, Atlanta, GA 30322, USA

[6]Department of Biomedical Sciences, College of Life and Health Sciences, Chubu University, Kasugai, Aichi 487-8501, Japan

[7]Center of Research Network for Infectious Diseases, Riken, Chiyoda-ku, Tokyo 100-0006, Japan

Infection of rhesus macaques with a deglycosylation mutant, Δ5G, derived from SIV239, a pathogenic clone of simian immunodeficiency virus (SIV), led to robust acute-phase viral replication followed by a chronic phase with undetectable viral load. This study examined whether humoral responses in Δ5G-infected animals played any role in the control of infection. Neutralizing antibodies (nAbs) were elicited more efficiently in Δ5G-infected animals than in SIV239-infected animals. However, functional nAb measured by 90% neutralization was prominent in only two of the five Δ5G-infected animals, and only at 8 weeks post-infection (p.i.), when viral loads were already below 10^4 copies ml^{-1}. These results suggest a minimal role for nAbs in the control of the primary infection. In contrast, whilst Ab responses to epitopes localized to the variable loops V1/V2 were detected in all Δ5G-infected animals at 3 weeks p.i., this response was associated with a concomitant reduction in Ab responses to epitopes in gp41 compared with those in SIV239-infected animals. These results suggest that the altered surface glycosylation and/or conformation of viral spikes induce a humoral response against SIV that is distinct from the response induced by SIV239. More interestingly, whereas V1/V2-specific Abs were induced in all animals, these Abs were associated with vigorous Δ5G-specific virion capture ability in only two Δ5G-infected animals that exhibited a functional nAb response. Thus, whereas the deglycosylation mutant infection elicited early virion capture and subsequent nAbs, the responses differed among animals, suggesting the existence of host factors that may influence the functional humoral responses against human immunodeficiency virus/SIV.

Received 25 May 2007
Accepted 7 October 2007

INTRODUCTION

The precise role of antibody (Ab) responses in the containment of human immunodeficiency virus (HIV) remains a subject of intense study and debate. Besides the classical direct virus neutralization properties, antibodies are also capable of blocking infection via other pathways such as antibody-dependent complement-mediated inactivation of virus (Aasa-Chapman *et al.*, 2005) and antibody-dependent cellular lysis (Ahmad & Menezes, 1996; Forthal *et al.*, 2001). Acquiring an understanding of these various mechanisms for their exploitation in the

development of candidate vaccines has been a major challenge.

The envelope protein (Env) of HIV/simian immunodeficiency virus (SIV) comprises an exterior protein (gp120) and a transmembrane (TM) protein (gp41), and trimers of the gp120/gp41 complexes form viral spikes that promote binding to receptors and co-receptors on the cell membrane for entry into the target cells (Wyatt & Sodroski, 1998). The major viral receptors of HIV/SIV include CD4 and a variety of co-receptors such as CCR5 or CXCR4. One desirable target epitope for neutralizing antibody (nAb) that shows relative conservation across clades is the binding site for the co-receptor (Burton *et al.*, 2004; Zolla-Pazner, 2004); however, this site is conformationally cryptic within the viral spike up until immediately after binding of the viral spike to CD4, providing an effective shielding mechanism to the virus. Another distinct feature of HIV/SIV Env is the extensive glycosylation that also effectively prevents access to antibodies directed at the epitopes (Chen *et al.*, 2005; Wyatt & Sodroski, 1998; Wyatt *et al.*, 1998). The gp120 protein possesses 18–33 Asn–X–Ser/Thr sequences, signals for the attachment of *N*-linked carbohydrate side chains (Leonard *et al.*, 1990; Ohgimoto *et al.*, 1998; Regier & Desrosiers, 1990; Zhang *et al.*, 2004). As the carbohydrate moiety is generally weakly immunogenic and is recognized to a large extent as self by the host immune system, the massive glycans on the surface of viral spikes constitute an immunologically silent facade (Wyatt & Sodroski, 1998; Wyatt *et al.*, 1998). As a result, mature viral spikes are protected from nAb and other host immune responses by a massive carbohydrate 'glycan shield' (Chen *et al.*, 2005; Wyatt & Sodroski, 1998; Wyatt *et al.*, 1998). In fact, a prominent role of carbohydrates of HIV/SIV in evasion from immune surveillance has been reported previously as follows. Variants of SIV that have evolved to acquire additional glycans in the variable regions of Env have increased neutralization resistance compared with the parental virus (Chackerian *et al.*, 1997; Cheng-Mayer *et al.*, 1999). Similarly, the appearance of neutralization escape mutants has been associated with altered glycosylation in HIV-1 evolved during the course of infection (Wei *et al.*, 2003). Conversely, infection with SIV239 mutants with deglycosylated Env (lacking *N*-linked glycosylation sites) in the variable loops V1/V2 of gp120 elicited markedly increased titres of nAb (Reitter *et al.*, 1998). We have reported that a deglycosylation mutant, Δ5G, lacking *N*-linked glycosylation sites at aa 79, 146, 171, 460 and 479 in gp120 of SIV239 displayed an attenuated phenotype when used to infect rhesus macaques (Mori *et al.*, 2001; Ohgimoto *et al.*, 1998). In addition, animals infected with Δ5G exhibited almost sterile protection against rechallenge with SIV239 (Mori *et al.*, 2001).

Thus, we suggest that studies aimed at identifying the mechanisms underlying the early and potent immune control of deglycosylated SIV may provide knowledge for the formulation of effective HIV/SIV vaccines. Studies performed herein were therefore directed at attempts to define more precisely the early humoral responses (both virus-specific nAb and non-nAb) generated after infection with Δ5G in rhesus macaques and to compare these responses with those observed in macaques inoculated with wild-type SIV239, with the rationale that results from such studies may help to identify their potential contribution towards viral control of primary infection.

METHODS

Viruses. The molecular pathogenic clone of SIV239 (Regier & Desrosiers, 1990) and its derived deglycosylated mutant, Δ5G, were used in this study. Δ5G was derived by mutagenesis of an SIV239 infectious DNA clone so that the asparagine residues for *N*-glycosylation at aa 79, 146, 171, 460 and 479 in gp120 were converted to glutamine residues (Fig. 1a) (Ohgimoto *et al.*, 1998). Viral stocks of SIV239 and Δ5G were prepared as reported previously (Mori *et al.*, 2001).

Peptides. A series of 72 consecutive 25 mer peptides overlapping by 13 aa were synthesized based on the entire SIV239 Env sequence (Env-1–72). These peptides were synthesized by the Microchemical Facility, Emory University School of Medicine, Atlanta, USA. Another set of 15 mer peptides overlapping by 11 aa around the V1/V2 region in gp120 (V1V2-1–12) was synthesized by Sigma-Aldrich Japan based on the Δ5G sequence (see Fig. 5b). All peptides were dissolved in DMSO diluted in PBS.

Animal infection. Juvenile rhesus macaques originating from Myanmar (Burma) (Mm12, Mm13, Mm20, Mm23 and Mm26) or from Laos (Mm07, Mm22 and Mm25) were used following the results of screening for SIV, simian T-cell lymphotropic virus, B virus and type D retrovirus infection, which were all negative prior to inception of the study. All animals were housed in individual cages and maintained according to the rules and guidelines for experimental animal welfare as outlined by the National Institute of Infectious Diseases and National Institute of Biomedical Innovation. Animals were infected intravenously with Δ5G or SIV239 as described previously (Mori *et al.*, 2001).

Plasma viral load measurements. SIV infection was monitored by measuring the plasma viral RNA load using a highly sensitive quantitative real-time RT-PCR. Viral RNA was isolated from plasma samples from infected animals using a commercial viral RNA isolation kit (Roche Diagnostics). SIV *gag* RNA was amplified and quantified using a method originally developed by Hofmann-Lehmann *et al.* (2000) using a TaqMan EZ RT-PCR kit (Applied Biosystems). The detection sensitivity of plasma viral RNA by this method was 100 viral RNA copies per ml plasma (given as copies ml^{-1}).

Neutralization assay. SIV neutralization was tested according to a protocol using CEMx174/SIVLTR-SEAP cells, originally described by Means *et al.* (1997). To measure low levels of nAb, IgG was purified from plasma as described below and concentrated virus stocks were used.

Anti-gp120 Ab ELISA and anti-Env peptide ELISA. Recombinant SIV239 gp120 and Δ5G gp120 were expressed utilizing a Sendai virus vector as described previously (Mori *et al.*, 2005; Yu *et al.*, 1997). Culture supernatant containing approximately 2 μg secreted SIV gp120 ml^{-1} was diluted with an equal amount of PBS, dispensed into each well of an ELISA plate and allowed to incubate at 4 °C overnight.

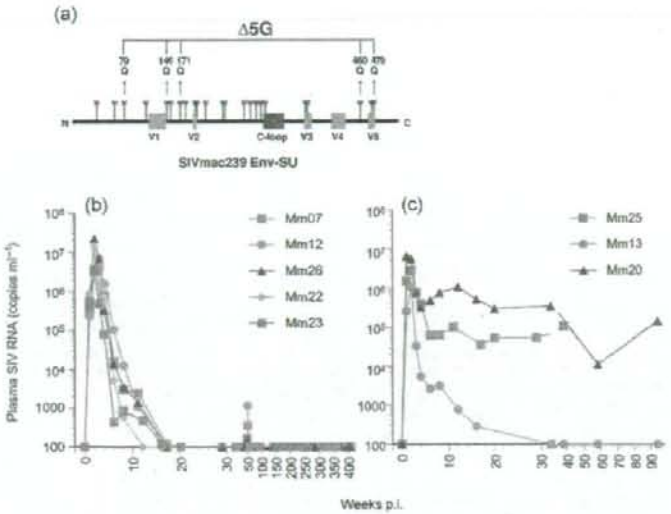

Fig. 1. Plasma SIV RNA loads in animals infected with Δ5G or SIV239. (a) *N*-Glycosylation sites in SIV239 gp120 and deglycosylation sites in Δ5G gp120. The locations of 23 *N*-glycosylation sites in SIV239 gp120, variable regions (V1–V5) and cysteine loops (C-loop) are shown. Δ5G was deglycosylated by N→Q substitutions at aa 79, 146, 171, 460 and 479 in Env (Ohgimoto *et al.*, 1998). (b, c) Plasma viral load in Δ5G-infected (b) and SIV239-infected (c) animals was measured in plasma samples using sensitive real-time RT-PCR to indicate when viral loads declined below 100 copies ml^{-1}. Three Δ5G-infected animals (Mm07, Mm12 and Mm26) were challenged with SIV239 at 48 weeks p.i.; thus, slightly increased viral loads were detected in those animals during weeks 49–51 p.i. (Mori *et al.*, 2001).

For the peptide ELISA, each peptide was diluted to 0.5 μM with 50 mM carbonate buffer (pH 9.5) and captured on Nunc Immobilizer amino plates (Nalge Nunc) at 4 °C overnight. A 1:100 dilution (150 μl) of the plasma sample to be tested was dispensed into antigen-immobilized plates and incubated at 37 °C for 1 h. Ab responses were detected using peroxidase-conjugated goat anti-monkey IgG and *o*-phenylenediamine. Absorbance was measured at 490 nm.

Removal of linear V1/V2 epitope-specific Abs from IgG fractions. A mixture of the peptides (V1V2-9, -10 and -11; see Fig. 5b) was conjugated to a HiTrap NHS-activated HP column (GE Healthcare). IgGs from plasma samples were fractionated using a mAb trap kit (GE Healthcare) and applied to the peptide-conjugated column. The flow-through fractions devoid of anti-V1V2-9, -10 and -11 peptide-specific Abs were collected. The concentration of IgG was determined using a protein assay kit (Bio-Rad).

Virion capture assay. The virion capture assay was modified using a method reported by Nyambi *et al.* (1998). ELISA plates were coated with the IgG samples described above at a concentration of 20 μg ml^{-1} in 50 mM carbonate buffer (pH 9.5) and incubated at 4 °C for 48 h. The plates were washed three times with PBS and blocked with 3 % BSA in PBS at 37 °C for 1 h. The plates were then washed three times with serum-free RPMI 1640. Δ5G or SIV239 virion solutions with a $p27^{Gag}$ concentration of 15, 7.5 and 3.75 ng in 10 % fetal bovine serum/RPMI 1640 were added to each well of the IgG-coated plate and incubated at 37 °C for 3 h. The wells were washed five times with serum-free RPMI 1640 to remove unbound virus. The virus bound to IgG was lysed using MagNA Pure LC Lysis/Binding Buffer (Roche Diagnostics). The viral lysates were subjected to viral RNA purification using a MagNA Pure Compact nucleic acid purification kit (Roche Diagnostics). The copy number of the isolated SIV RNA was determined by real-time RT-PCR for SIV239 as described above.

Statistical analysis. Correlation analysis was done using Spearman's non-parametric rank test and the Mann–Whitney test using GraphPad Prism 4.0 software. Correlations were considered to be statistically significant for values of $P<0.05$.

RESULTS

Plasma viral loads of a quintuple deglycosylated SIV239 mutant in rhesus macaques

Eight rhesus macaques were infected intravenously with Δ5G ($n=5$) or SIV239 ($n=3$) (Mori *et al.*, 2001). Plasma viral RNA loads were assayed for up to 400 weeks p.i. and the data obtained in the Δ5G-infected (Fig. 1b) or SIV239-infected (Fig. 1c) animals were plotted. Both Δ5G and SIV239 replicated with similar kinetics during the early phase of primary infection for up to 4 weeks p.i. However, subsequent to this acute infection phase, virus replication was markedly different in the two groups of monkeys: SIV239-infected animals exhibited viral load set points around 10^5 copies ml^{-1} in two of three animals, with one animal (Mm13) having an undetectable viral load (<100 copies ml^{-1}) by 30 weeks p.i. (Fig. 1c). In contrast, the Δ5G-infected animals showed uniformly controlled viraemia reaching undetectable levels by 12–16 weeks p.i. and maintained this control for more than 6 years p.i. (Fig. 1b).

nAb response in Δ5G-infected animals

Although failure to detect a nAb response is characteristic of SIV239-infected rhesus macaques (Johnson *et al.*, 2003; Means *et al.*, 1997), the rapid control of viraemia in Δ5G-infected animals prompted us to determine whether nAb played a role in this control of viraemia. We hypothesized that the deglycosylation might lead to the elicitation of a markedly more vigorous nAb response than infection with SIV239. To maximize the detection sensitivity of weak nAb responses at early time points p.i., an assay that measures neutralization titres based on 50 % inhibition of virus replication (IC_{50}) in $CD4^+$ T-cell lines was initially used.

Consistent with the reported results in SIV239-infected animals, no appreciable nAb titre was detected in two animals (Mm13 and Mm25), despite the fact that viral load in Mm13 was distinctively decreased by 30 weeks p.i. However, we observed a rare animal (Mm20) that elicited a robust nAb response against SIV239 and a relatively delayed nAb response against Δ5G, despite the maintenance of a high viral load (Fig. 2a). These results indicated the lack of correlation of nAb response with viral load in SIV239-infected animals. In contrast, nAb was detected in two Δ5G-infected animals (Mm07 and Mm22) starting at 8 weeks p.i. and in two additional animals (Mm12 and Mm23) at 12 weeks p.i. (Fig. 2b, left panel). These titres peaked at either 12 or 18 weeks p.i., and the peak was followed by a decrease in titre that varied among animals. Mm12 and Mm23, which exhibited nAb induction at 12 weeks p.i., had essentially low titres, whilst Mm07 and Mm22, which exhibited nAb induction at an earlier time point, maintained vigorous nAb titres of >1 : 100. Of note, plasma from Mm26 did not contain detectable levels of nAb at any time p.i. In contrast, nAb against SIV239 was not induced in any of the Δ5G-infected animals (Fig. 2b, right panel). As low-level nAb may play a role in control of virus replication, purified IgG from the plasma samples was used to measure neutralizing activity. However, the results from the purified IgG corresponding to the plasma at a 1 : 3 dilution did not change the kinetics of nAb response in Δ5G-infected animals (data not shown).

In experiments where the passive administration of monoclonal HIV nAb successfully prevented the infection of macaques with simian–human immunodeficiency virus, the results unequivocally indicated that high titres of nAb were needed to achieve such protection (Nishimura *et al.*, 2002). In consideration of these results, data were recalculated based on a cut-off value of 90 % inhibition of virus replication (IC_{90}) in $CD4^+$ T-cell lines. As a result, nAb responses were detected in only two of the animals, Mm07 and Mm22, but with titres of 1 : 100 and 1 : 500, respectively (Fig. 2b, middle panel). Next, we examined the correlation between viral load and nAb titre at 8 and 12 weeks p.i. and found that the correlation was not statistically significant (Fig. 2c).

Anti-gp120 Ab response in Δ5G-infected animals

Next, we measured binding Ab responses against gp120. When the plasma samples were assayed for levels of Ab that bound to SIV239 gp120 or Δ5G gp120, essentially identical values were obtained. Fig. 3 shows the data obtained using SIV239 gp120. Remarkably, anti-gp120 responses during the early period p.i. between the two groups of monkeys were distinct. Whereas anti-gp120-specific Ab responses

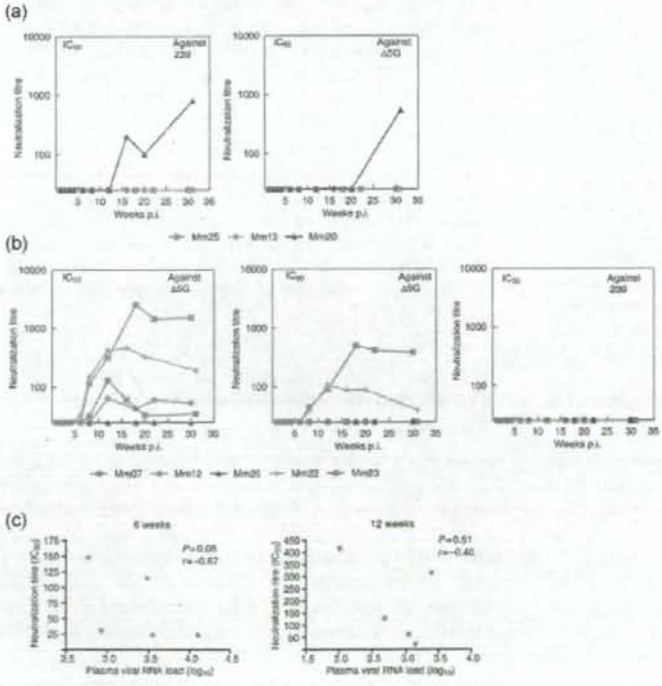

Fig. 2. nAb titres in SIV-infected animals. (a) nAb titres in SIV239-infected animals are indicated as the plasma dilution yielding 50 % inhibition (IC_{50}) of SIV239 infection (left) or Δ5G infection (right) in CEMx174/SIVLTR-SEAP cells. (b) nAb titres in Δ5G-infected animals are indicated as the plasma dilution that yielded 50 % inhibition (IC_{50}, left) and 90 % inhibition (IC_{90}, middle) of Δ5G infection or 50 % inhibition of SIV239 infection (right) in CEMx174/SIVLTR-SEAP cells. (c) Correlation between IC_{50} nAb titres and plasma viral RNA load at 8 and 12 weeks p.i. in Δ5G-infected animals.

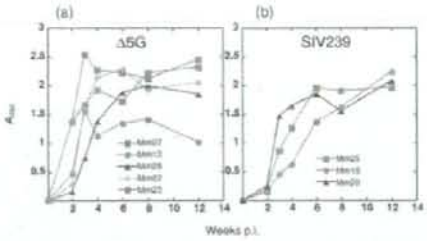

Fig. 3. Anti-gp120 Ab responses. Anti-gp120 Ab responses in Δ5G-infected (a) and SIV239-infected (b) animals were indicated as A_{490} using plasma diluted 1 : 100 in an ELISA.

peaked at 3–4 weeks p.i. in Δ5G-infected animals (Fig. 3a), those in SIV239-infected animals remained generally lower and required longer periods of time to reach their peak (Fig. 3b). Of note, whilst anti-gp120 Ab responses did not correlate well with nAb titres in the chronic phase in Δ5G-infected animals, the hierarchy detected in nAb titres (Mm07, Mm22, Mm23, Mm12 and Mm26, in descending order) was similar to that observed for gp120-binding antibodies at 2 weeks p.i. (Fig. 3a).

Ab responses to linear epitopes in gp120 and gp41 in Δ5G-infected animals differ from those detected in SIV239-infected animals

Next, we examined Ab-binding responses to linear epitopes in plasma samples from infected animals at 8 weeks p.i., as both nAb and anti-gp120-binding Ab were detected at this time point (Figs 2 and 3). We used 72 overlapping peptides encompassing the entire Env sequence of SIV239 for the detection of epitope-specific Ab in plasma samples from Δ5G-infected or SIV239-infected animals. As shown in Fig. 4 and Table 1, the plasma samples reacted with the peptides in six regions: two in gp120 and four in gp41. The regions in gp120 resided in the vicinity of V1/V2, designated region 1 (aa 109–193), and at the C terminus, designated region 2 (aa 493–529). Of note, only linear region 1 was directly affected by selected deglycosylation (aa 146 and 171). The regions in gp41 were located in the ectodomain for region 3 (aa 589–625) and region 4 (aa 660–685), and in the cytoplasmic domain for region 5 (aa 721–757) and region 6 (aa 841–879).

Although Ab responses to most of the peptides recognized in the plasma samples from Δ5G-infected animals were similar to those in SIV239-infected animals, a few peptides were recognized by Abs only in samples from Δ5G-infected animals, and Ab reactivity to some peptides was significantly different between the two groups (Fig. 4b, c and Table 1). Firstly, in region 1, whereas five peptides (Env-10, -12, -13, -14 and -15) were recognized by Abs from Δ5G-infected animals, only three peptides (Env-10, -12 and -13) reacted with Abs from SIV239-infected animals (Fig. 4b and c). Peptide Env-10 was detected by Abs from four Δ5G-infected animals, but from only one of the SIV239-infected animals. Similarly, peptides Env-12 and -13 were detected by Abs from five Δ5G-infected animals and two SIV239-infected animals. In contrast, peptides Env-14 and -15 were detected by Abs from Δ5G-infected animals but not SIV239-infected animals. The specificity of Δ5G infection in the reactivity of peptide Env-14 was statistically significant (P=0.0149) (Table 1). Secondly, the reactivity of Ab from Δ5G-infected animals with the peptides in regions 2, 3 and 4 was lower than that recorded with Ab from SIV239-infected animals (Fig. 4b and c). As shown in Table 1, the reduction in Ab reactivity from Δ5G-infected animals to peptide Env-51 (region 3) and peptide Env-56 (region 4) was significant (P=0.014 and 0.0053, respectively); however, the reduction in Ab response in region 2 was not significant. In addition, there were no significant differences in the Ab responses to the peptides in regions 5 and 6 between Δ5G-infected and SIV239-infected monkeys (Fig. 4b, c and Table 1).

A Δ5G-specific linear epitope resides in the region containing the third deglycosylation site (aa 171) between V1 and V2

As region 1 also contained the site of two mutations introduced to limit glycosylation in the Δ5G mutant, we focused additional studies on this region. To identify the Δ5G-specific epitope(s) in region 1, peptide ELISA was performed with 12 newly synthesized shorter peptides based on the Δ5G sequence spanning the V1/V2 region (Fig. 5). Ab reactivity to peptide Env-14 was mapped to peptides V1V2-9–11 (Fig. 5a). Thus, three linear epitopes (encompassed in peptides Env-10, V1V2-3 and V1V2-9–11) were identified within the V1/V2 region (Figs 4 and 5). Whilst two epitopes contained in peptides Env-10 and V1V2-3 were recognized by Ab from both SIV239- and Δ5G-infected animals, the epitope(s) corresponding to peptides V1V2-9–11 was specific to Δ5G infection (Fig. 5a). As the latter contained the third deglycosylation mutation (Figs 1 and 5b, aa 171), Δ5G specificity was probably secondary to the removal of *N*-glycan at this site in SIV239 gp120 (Fig. 5).

Δ5G-specific Ab responses to linear epitopes in Env elicited immediately following primary infection

In an effort to define the potential relevance of the linear epitope-specific Ab responses in the reduction of acute virus replication in Δ5G-infected animals, we examined the kinetics of Ab reactivity to 12 peptides: Env-10, V1V2-3 and V1V2-9, -10 and -11 for epitopes in region 1; Env-42 and -43 for epitopes in region 2; Env-50 and -51 for epitopes in region 3; Env-56 for epitopes in region 4; and Env-61 and -62 for epitopes in region 5 (Fig. 6). Whilst the induction kinetics of Ab to most peptides were variable in

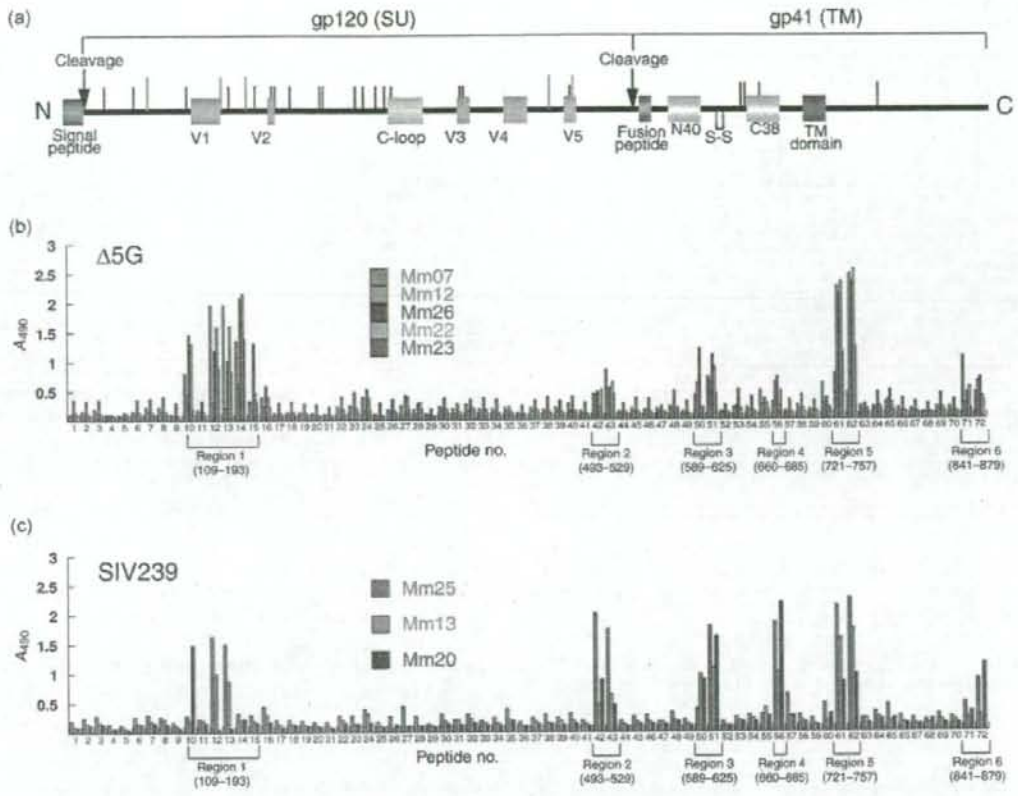

Fig. 4. Ab reactivity to synthetic overlapping peptides spanning the entire Env protein. (a) Diagram of SIV239 Env with the locations of the signal peptide (violet box), variable regions (pink boxes), cysteine loop (yellow box), fusion peptide (green box), N-terminal (N40) and C-terminal (C38) heptad repeats (light-blue boxes), membrane-spanning domain (blue box) and *N*-glycosylation sites (vertical bars) (Burns & Desrosiers, 1991; Choi *et al.*, 1994; Liu *et al.*, 2002). Red vertical bars indicate deglycosylation sites (aa 79, 146, 171, 460 and 479) in Δ5G. S-S indicates the indispensable disulfide bond for hairpin loop formation of the TM protein. (b, c) Plasma samples collected from animals infected with Δ5G (b) and SIV239 (c) at 8 weeks p.i. were used to examine Ab reactivity to 72 peptides (25 mers) overlapping by 13 residues each and spanning the entire Env protein. Reactivity was shown by A_{490}.

plasma from both groups of animals, Ab to V1V2-9, -10 and -11 was specific for Δ5G-infected animals, with rapid induction following primary infection. Ab responses to Env-61 and -62 were also induced rapidly in animals from the two groups; however, it has already been confirmed by SIV and HIV studies that a linear epitope covered by these peptides is the immunodominant epitope with no association with virus control (Eberle *et al.*, 1997; Kent *et al.*, 1992). In contrast to Ab responses to V1/V2 peptides, whilst Ab to peptides Env-51 and -56 in the gp41 ectodomain were detected in SIV239-infected animals, these reactions were low until at least 12 weeks p.i. in Δ5G-infected animals.

Properties of Ab against Δ5G-specific linear epitope

Although Ab reactivity to peptide V1V2-9, -10 and -11 was elicited specifically in Δ5G-infected animals, these Abs were non-nAbs, as these binding Abs were detected in all Δ5G-infected animals, including a nAb-undetectable monkey (Mm26), and before nAb was detected. In addition, we attempted to inhibit neutralization by the addition of excess concentrations of V1V2-9, -10 and -11 to the neutralization assay performed with plasma from Δ5G-infected animals collected at 8 and 12 weeks p.i. The reduction of nAb by the addition of an excess amount of

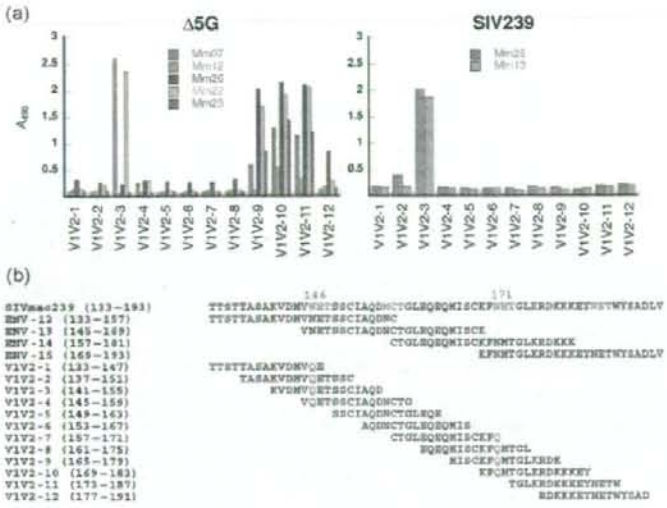

Fig. 5. Ab reactivity to linear epitopes in the V1/V2 region of gp120. (a) To define linear epitopes in the V1/V2 region, peptide ELISA was performed using 12 peptides (15 mers) overlapping by 11 residues each. (b) Sequences and positions of the 12 V1/V2 peptides used in (a) and the peptides Env-12 to -15.

peptide was not detected in any samples, confirming that the epitopes targeted by nAb and V1V2-specific Ab were distinct (data not shown).

Next, we tested plasma IgG samples from SIV-infected animals for the quantitative capture of whole virions. IgG fractions of plasma samples from SIV-infected animals collected at 3–4 weeks p.i. were compared for their capacity to capture Δ5G or SIV239 virions. IgG fractions from two Δ5G-infected animals (Mm07 and Mm22) exhibited remarkably higher virion capture activity than those from other animals (Fig. 7a); however, this capture activity was

Table 1. Epitope-specific Ab-binding regions in Env and influence of deglycosylation on Ab binding

Env subunit	Ab-binding region	Peptide no.	Amino acid range	Region	*P* value*
SU	Region 1	10	109–133	V1	0.6733
		12	133–157	V1	0.5678
		13	145–169	V1/V2	0.5563
		14	157–181	V1/V2	0.0149†
		15	169–193	V1/V2	0.2385
	Region 2	42	493–517	SU C terminus	0.0822
		43	505–529		0.3039
TM	Region 3	50	589–613	Ectodomain	0.4791
		51	601–625		0.0140†
	Region 4	56	660–685	Ectodomain	0.0053‡
	Region 5	61	721–746	Cytoplasmic domain	0.6818
		62	732–757		0.8188
	Region 6	71	841–865	Cytoplasmic domain	0.5237
		72	853–879		0.2451

*A *t*-test was performed by using data in Fig. 4 to determine differences in Ab reactivity between SIV239 infection and Δ5G infection.
†$P<0.05$; ‡$P<0.01$.

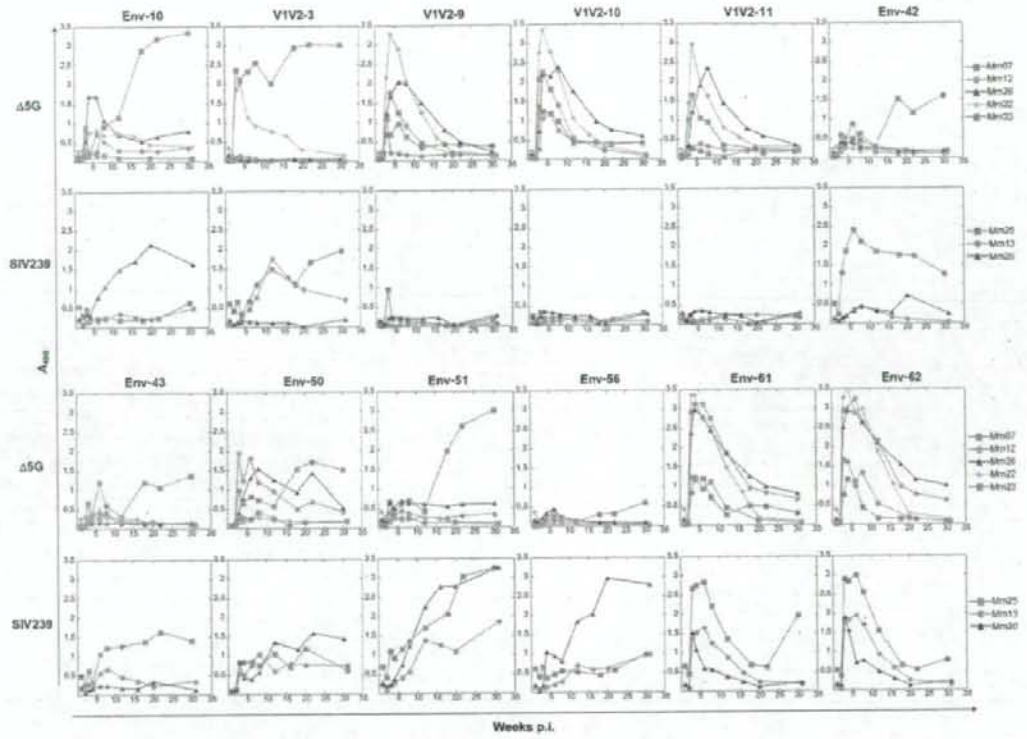

Fig. 6. Kinetics of peptide-specific Ab responses in Δ5G-infected and SIV239-infected animals. The kinetics of Ab reaction against peptides selected in the experiments shown in Figs 4 and 5 was determined as A_{490} using plasma diluted 1 : 100 in an ELISA.

Δ5G-specific, as no appreciable capture of SIV239 virion was detected with these samples. Furthermore, this activity was reduced to the level of control IgG (R374) after selective removal of IgG binding to V1V2-9, -10 and -11 peptides, suggesting that virion capture activity is associated with the Δ5G-specific linear epitope Ab (Fig. 7a). By contrast, IgG fractions from SIV239-infected animals collected at 3–4 weeks p.i. did not exhibit appreciable binding activity either to Δ5G virions or SIV239 virions (Fig. 7b). Thus, these results demonstrated that Δ5G infection elicited not only nAb after 8 weeks p.i., but also a much earlier humoral antiviral mechanism in the form of Δ5G-specific virion-binding Ab at 3–4 weeks p.i. in at least two monkeys (Mm07 and Mm22). To examine the relationship between the two antibody activities, we calculated the correlation of virion capture activity of IgG at 3 or 4 weeks p.i. with a peak nAb titre in Δ5G-infected animals (Fig. 2b) and found that this correlation was statistically significant (r=1, P=0.0167; Fig. 7c).

DISCUSSION

nAb response in Δ5G-infected animals

Glycosylation of viral spikes has long been recognized as an effective strategy to evade host (humoral) immune surveillance for several pathogens and for HIV/SIV in particular (Dowling *et al.*, 2007; Fournillier *et al.*, 2001; Haigwood & Stamatatos, 2003; Huso *et al.*, 1988; Reitter *et al.*, 1998). In support of these observations, the data presented here demonstrated that quintuple deglycosylation conferred live attenuated vaccine properties to an SIV239 mutant, Δ5G (Mori *et al.*, 2001); however, a cellular but not humoral response was detected as an immune correlate of the protection of Δ5G-infected animals against SIV239 challenge infection. Therefore, we assumed that the complete control of robust acute virus replication in Δ5G-infected animals beyond the initial cell-mediated control would be due to the development of rapid and effective nAbs. This study indicated that, whereas

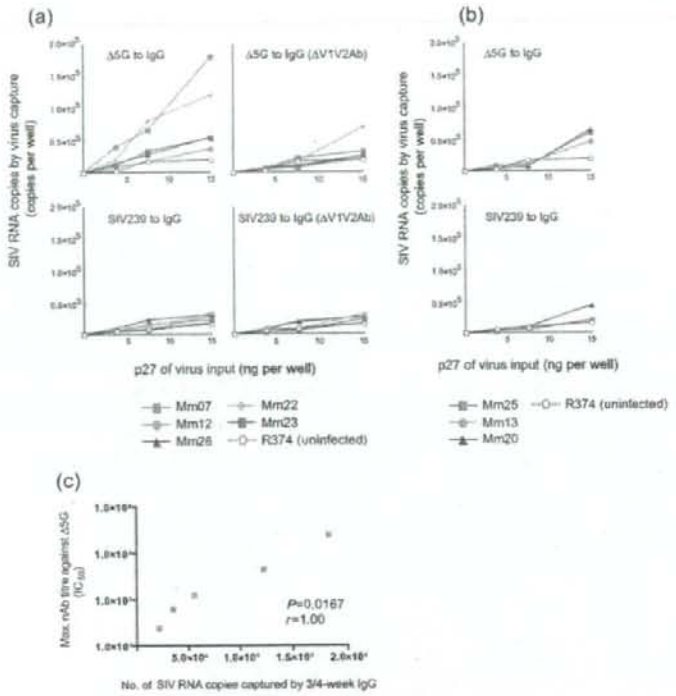

Fig. 7. Virion capture activity of IgG from Δ5G-infected and SIV239-infected animals. Virion capture activity of IgG from the plasma of infected animals at 3 or 4 weeks p.i. was determined by increased captured SIV RNA relative to input (3.75, 7.5 and 15 ng $p27^{gag}$) of Δ5G or SIV239. Plasma samples of Δ5G-infected animals (a) and SIV239-infected animals (b) were used for the assay. IgG (ΔV1V2Ab) indicates IgG depleted of Ab binding to V1V2-9, -10 or -11 peptide. R374 was an uninfected monkey. Correlation between virion capture activity at 3 or 4 weeks p.i. and peak nAb titre in Δ5G-infected animals (Fig. 2b) is shown (c).

Δ5G-infected animals clearly exhibited better nAb responses than SIV239-infected animals, the most stringent nAb assay, based on 90 % inhibition, provided evidence of nAb titres in only two of five Δ5G-infected animals and the appearance of these titres trailed the decline of acute viral loads by almost 4 weeks (Figs 1 and 2). Therefore, we concluded that, although deglycosylation did promote better development of nAbs in Δ5G-infection than SIV239 infection, it was still too late to control acute viraemia.

Zinkernagel and co-workers have categorized viruses into two types: 'acutely cytopathic viruses' and 'poorly or non-cytopathic viruses' (Hangartner *et al.*, 2006b). The former contains viruses such as vesicular stomatitis virus in mice and influenza virus in humans, whose control depends primarily on a rapid and potent nAb response. The latter comprises viruses such as lymphocytic choriomenigitis virus in mice, and hepatitis B and C viruses and HIV in humans, against which a nAb response is apparent only following the reduction of primary viraemia, and which establish persistent chronic infections. Accordingly, although the viral loads in Δ5G infection resembled 'acutely cytopathic virus' infections, the kinetics of nAbs still conformed to the 'non-cytopathic virus' category. As the difference in nAb response between the two types of virus is determined by their surface glycoproteins (Pinschewer *et al.*, 2004), this study suggests that the deglycosylation of Δ5G could not change this intrinsic property of SIV239.

Ab responses to Env peptides in Δ5G-infected animals

Aside from nAb, non-nAb responses to linear epitopes in V1/V2 were specifically induced by 3 weeks p.i. in all Δ5G-infected animals (Figs 4, 5 and 6). The heavy glycosylation of viral spikes clearly prevented access of B-cell receptors to the linear Ab epitopes located within limited regions of gp120 in SIV239, and the reduced glycosylation probably promoted better exposure of these linear epitopes in Δ5G (Fig. 4). Accordingly, the Δ5G-specific epitope in V1/V2 should be closely associated with the deglycosylation mutation at aa 171 in gp120 (Fig. 5). We speculate that this Ab induction might contribute to acute viral suppression in Δ5G infection because of the coincident decrease in peak viraemia (Figs 1 and 6). Non-neutralizing Abs can be divided into those that bind to the intact virion surface and debris-specific Ab. The former non-neutralizing Abs have occasional possibilities for antiviral activities such as antibody-dependent cell-mediated cytotoxicity and complement-mediated virus inactivation (Aasa-Chapman *et al.*, 2005; Ahmad & Menezes, 1996; Forthal *et al.*, 2001; Hangartner *et al.*, 2006a). In fact, readily detectable virion

capture Abs were induced in two of five Δ5G-infected animals (Fig. 7, Mm07 and Mm22). The importance of immediate-early suppression of SIV replication for the long-term containment of infection has been demonstrated by studies of post-exposure anti-retroviral therapy (Lifson *et al.*, 2000; Mori *et al.*, 2000). Thus, the early and complete control of viraemia in Δ5G-infected animals clearly suggests an antiviral mechanism(s) acting as early as 2–4 weeks p.i. Therefore, the early detection of IgG capable of virus capture in Δ5G-infected animals may provide mechanisms capable of contributing to undetectable viral load set points (Fig. 1b). The selective generation of such Ab directed to linear Env epitopes is expected.

Interestingly, deglycosylation in gp120 was also associated with a general reduction in the antigenicity of linear epitopes in gp41: the Ab response against the two epitopes that reside in the regions between the two heptad repeats (aa 601–625) and in the C-terminal heptad repeat (aa 660–685), respectively, was markedly reduced (Fig. 4, Table 1). The former corresponds to the highly conserved immunogenic epitope (Benichou *et al.*, 1993; Gnann *et al.*, 1987; Silvera *et al.*, 1994), and the latter corresponds to an epitope identified in the chronic phase of SIVmac251 infection (Silvera *et al.*, 1994) and corresponds to the nAb epitope of HIV-1 known as 2F5 (Muster *et al.*, 1993), although this linear epitope has not been associated with SIV neutralization (Caffrey *et al.*, 1998). Thus, these epitopes are probably exposed on the surface of viral spikes or their degraded fragments in most SIV and HIV-1 isolates with appropriate glycosylation and correct folding. We believe that the loss of glycosylation might induce a slight conformational change in the gp120 protein backbone, resulting in altered interaction of gp120 and gp41. In fact, the region encompassing the former epitope in gp41 was demonstrated to interact with gp120 (Cao *et al.*, 1993; Maerz *et al.*, 2001; York & Nunberg, 2004). As viral spikes determine virus properties such as viral receptor usage and cell tropism (Kolchinsky *et al.*, 2001; Puffer *et al.*, 2002), different cell populations might be infected in Δ5G-infected animals compared with SIV239 infection. More specifically, because of the distinct properties of the virus, vigorous Δ5G replication in the acute phase did not apparently impair immune function and thus established the control of chronic-phase infection and viral replication.

Host factors required for functional Ab responses against SIV infection

This study also demonstrated remarkable differences in humoral response with regard to nAb and virion capture Ab among Δ5G-infected animals. However, gp120-specific-binding Ab and the linear epitope-specific Ab were initially induced similarly in all animals. These findings imply that Abs measured by ELISA assay and Abs exhibiting antiviral activity are elicited by different pathways and that the properties associated with functional Abs depend largely on the host and underscore the importance of its genetic background. Rhesus macaques are present in various geographical locations within the Asian continent and are subdivided into many subspecies morphologically and genetically (Smith & McDonough, 2005). Some of the genetic differences among rhesus monkeys of different geographical origins, and especially those involving major histocompatibility complex (MHC) genotypes, probably influence the corresponding differences in immune responses, especially cellular response (Bontrop *et al.*, 1996; O'Connor *et al.*, 2003; Reimann *et al.*, 2005). Schmitz *et al.* (2005) reported that Mamu-A*01-positive rhesus monkeys elicited a significantly higher cellular response and lower nAb titres than those in Mamu-A*01-negative animals at the time of challenge infection of animals vaccinated with live attenuated SIV. They suggested that both humoral and cellular immune responses contributed to the protection against the challenge infection and that the relative contribution of each of the responses may be genetically determined. We observed a similar relationship between nAb and cellular responses among Δ5G-infected animals: two animals (Mm07 and Mm22) elicited a lower cellular response while the other three animals (Mm12, Mm23 and Mm26) elicited a higher cellular response (data not shown). Notably two animals exhibiting highly functional Ab (Mm07 and Mm22) were the offspring of seed animals imported from Laos, whilst the others (Mm12, Mm23 and Mm26) were of Burmese origin, suggesting the potential association of such different humoral and cellular responses with host genetic factors. In clinical studies, considerable concordance of adaptive cellular and humoral responses and HIV evolution in monozygotic twins, but not in brothers, infected with the same virus has been reported (Draenert *et al.*, 2006). HIV-1-exposed but uninfected status with significantly higher neutralizing IgA was linked to genotypes on chromosome 22 (Kanari *et al.*, 2005). In the mouse Friend leukemia virus model, MHC II alleles were determined as host genetic factors required for effective nAb response (Miyazawa *et al.*, 1992) and the host genetic factor was mapped to chromosome 15, which was associated with the clearance of viraemia by nAb (Hasenkrug *et al.*, 1995; Kanari *et al.*, 2005).

Taken together, we speculate that the functional humoral response is determined by host genetic properties similar to the cellular immune response. Thus, gaining knowledge of the genetic requirements for both humoral and cellular containment of viral infections will clearly be of primary importance for vaccine development and therapeutics against HIV and other infectious agents.

NOTE ADDED IN PROOF

A discrepancy in the SIV239-infected animals Mm13 and Mm20 was noted between the result shown in Fig. 2 and that in a previous report Mori *et al.*, 2001. The nAb

response against SIV239 in Mm20 was confirmed at multiple time points in the present study.

ACKNOWLEDGEMENTS

We thank Kayoko Ueda for excellent technical assistance and Marcelo Kuroda for critical reading of the manuscript. This study was conducted through the Cooperative Research Program in the Tsukuba Primate Research Center, National Institute of Biomedical Innovation, Japan. This work was supported by AIDS research grants from the Health Sciences Research Grants, from the Ministry of Health, Labour and Welfare in Japan, and from the Ministry of Education, Culture, Sports, Science and Technology in Japan.

REFERENCES

Aasa-Chapman, M. M., Holuigue, S., Aubin, K., Wong, M., Jones, N. A., Cornforth, D., Pellegrino, P., Newton, P., Williams, I. & other authors (2005). Detection of antibody-dependent complement-mediated inactivation of both autologous and heterologous virus in primary human immunodeficiency virus type 1 infection. *J Virol* **79**, 2823–2830.

Ahmad, A. & Menezes, J. (1996). Antibody-dependent cellular cytotoxicity in HIV infections. *FASEB J* **10**, 258–266.

Benichou, S., Venet, A., Beyer, C., Tiollais, P. & Madaule, P. (1993). Characterization of B-cell epitopes in the envelope glycoproteins of simian immunodeficiency virus. *Virology* **194**, 870–874.

Bontrop, R. E., Otting, N., Niphuis, H., Noort, R., Teeuwsen, V. & Heeney, J. L. (1996). The role of major histocompatibility complex polymorphisms on SIV infection in rhesus macaques. *Immunol Lett* **51**, 35–38.

Burns, D. P. & Desrosiers, R. C. (1991). Selection of genetic variants of simian immunodeficiency virus in persistently infected rhesus monkeys. *J Virol* **65**, 1843–1854.

Burton, D. R., Desrosiers, R. C., Doms, R. W., Koff, W. C., Kwong, P. D., Moore, J. P., Nabel, G. J., Sodroski, J., Wilson, I. A. & Wyatt, R. T. (2004). HIV vaccine design and the neutralizing antibody problem. *Nat Immunol* **5**, 233–236.

Caffrey, M., Cai, M., Kaufman, J., Stahl, S. J., Wingfield, P. T., Covell, D. G., Gronenborn, A. M. & Clore, G. M. (1998). Three-dimensional solution structure of the 44 kDa ectodomain of SIV gp41. *EMBO J* **17**, 4572–4584.

Cao, J., Bergeron, L., Helseth, E., Thali, M., Repke, H. & Sodroski, J. (1993). Effects of amino acid changes in the extracellular domain of the human immunodeficiency virus type 1 gp41 envelope glycoprotein. *J Virol* **67**, 2747–2755.

Chackerian, B., Rudensey, L. M. & Overbaugh, J. (1997). Specific *N*-linked and *O*-linked glycosylation modifications in the envelope V1 domain of simian immunodeficiency virus variants that evolve in the host alter recognition by neutralizing antibodies. *J Virol* **71**, 7719–7727.

Chen, B., Vogan, E. M., Gong, H., Skehel, J. J., Wiley, D. C. & Harrison, S. C. (2005). Structure of an unliganded simian immunodeficiency virus gp120 core. *Nature* **433**, 834–841.

Cheng-Mayer, C., Brown, A., Harouse, J., Luciw, P. A. & Mayer, A. J. (1999). Selection for neutralization resistance of the simian/human immunodeficiency virus $SHIV_{SF33A}$ variant in vivo by virtue of sequence changes in the extracellular envelope glycoprotein that modify *N*-linked glycosylation. *J Virol* **73**, 5294–5300.

Choi, W. S., Collignon, C., Thiriart, C., Burns, D. P., Stott, E. J., Kent, K. A. & Desrosiers, R. C. (1994). Effects of natural sequence variation on recognition by monoclonal antibodies neutralize simian immunodeficiency virus infectivity. *J Virol* **68**, 5395–5402.

Dowling, W., Thompson, E., Badger, C., Mellquist, J. L., Garrison, A. R., Smith, J. M., Paragas, J., Hogan, R. J. & Schmaljohn, C. (2007). Influences of glycosylation on antigenicity, immunogenicity, and protective efficacy of Ebola virus GP DNA vaccines. *J Virol* **81**, 1821–1837.

Draenert, R., Allen, T. M., Liu, Y., Wrin, T., Chappey, C., Verrill, C. L., Sirera, G., Eldridge, R. L., Lahaie, M. P. & other authors (2006). Constraints on HIV-1 evolution and immunodominance revealed in monozygotic adult twins infected with the same virus. *J Exp Med* **203**, 529–539.

Eberle, J., Loussert-Ajaka, I., Brust, S., Zekeng, L., Hauser, P. H., Kaptue, L., Knapp, S., Damond, F., Saragosti, S. & other authors (1997). Diversity of the immunodominant epitope of gp41 of HIV-1 subtype O and its validity for antibody detection. *J Virol Methods* **67**, 85–91.

Forthal, D. N., Landucci, G. & Keenan, B. (2001). Relationship between antibody-dependent cellular cytotoxicity, plasma HIV type 1 RNA, and $CD4^+$ lymphocyte count. *AIDS Res Hum Retroviruses* **17**, 553–561.

Fournillier, A., Wychowski, C., Boucreux, D., Baumert, T. F., Meunier, J. C., Jacobs, D., Muguet, S., Depla, E. & Inchauspe, G. (2001). Induction of hepatitis C virus E1 envelope protein-specific immune response can be enhanced by mutation of *N*-glycosylation sites. *J Virol* **75**, 12088–12097.

Gnann, J. W., Jr, Nelson, J. A. & Oldstone, M. B. (1987). Fine mapping of an immunodominant domain in the transmembrane glycoprotein of human immunodeficiency virus. *J Virol* **61**, 2639–2641.

Haigwood, N. L. & Stamatatos, L. (2003). Role of neutralizing antibodies in HIV infection. *AIDS* **17** (Suppl. 4), S67–S71.

Hangartner, L., Zellweger, R. M., Giobbi, M., Weber, J., Eschli, B., McCoy, K. D., Harris, N., Recher, M., Zinkernagel, R. M. & Hengartner, H. (2006a). Nonneutralizing antibodies binding to the surface glycoprotein of lymphocytic choriomeningitis virus reduce early virus spread. *J Exp Med* **203**, 2033–2042.

Hangartner, L., Zinkernagel, R. M. & Hengartner, H. (2006b). Antiviral antibody responses: the two extremes of a wide spectrum. *Nat Rev Immunol* **6**, 231–243.

Hasenkrug, K. J., Valenzuela, A., Letts, V. A., Nishio, J., Chesebro, B. & Frankel, W. N. (1995). Chromosome mapping of *Rfv3*, a host resistance gene to Friend murine retrovirus. *J Virol* **69**, 2617–2620.

Hofmann-Lehmann, R., Swenerton, R. K., Liska, V., Leutenegger, C. M., Lutz, H., McClure, H. M. & Ruprecht, R. M. (2000). Sensitive and robust one-tube real-time reverse transcriptase-polymerase chain reaction to quantify SIV RNA load: comparison of one- versus two-enzyme systems. *AIDS Res Hum Retroviruses* **16**, 1247–1257.

Huso, D. L., Narayan, O. & Hart, G. W. (1988). Sialic acids on the surface of caprine arthritis-encephalitis virus define the biological properties of the virus. *J Virol* **62**, 1974–1980.

Johnson, W. E., Sanford, H., Schwall, L., Burton, D. R., Parren, P. W., Robinson, J. E. & Desrosiers, R. C. (2003). Assorted mutations in the envelope gene of simian immunodeficiency virus lead to loss of neutralization resistance against antibodies representing a broad spectrum of specificities. *J Virol* **77**, 9993–10003.

Kanari, Y., Clerici, M., Abe, H., Kawabata, H., Trabattoni, D., Caputo, S. L., Mazzotta, F., Fujisawa, H., Niwa, A. & other authors (2005). Genotypes at chromosome 22q12–13 are associated with HIV-1-exposed but uninfected status in Italians. *AIDS* **19**, 1015–1024.

Kent, K. A., Rud, E., Corcoran, T., Powell, C., Thiriart, C., Collignon, C. & Stott, E. J. (1992). Identification of two neutralizing and 8 non-neutralizing epitopes on simian immunodeficiency virus envelope

using monoclonal antibodies. *AIDS Res Hum Retroviruses* **8**, 1147–1151.

Kolchinsky, P., Kiprilov, E., Bartley, P., Rubinstein, R. & Sodroski, J. (2001). Loss of a single *N*-linked glycan allows CD4-independent human immunodeficiency virus type 1 infection by altering the position of the gp120 V1/V2 variable loops. *J Virol* **75**, 3435–3443.

Leonard, C. K., Spellman, M. W., Riddle, L., Harris, R. J., Thomas, J. N. & Gregory, T. J. (1990). Assignment of intrachain disulfide bonds and characterization of potential glycosylation sites of the type 1 recombinant human immunodeficiency virus envelope glycoprotein (gp120) expressed in Chinese hamster ovary cells. *J Biol Chem* **265**, 10373–10382.

Lifson, J. D., Rossio, J. L., Arnaout, R., Li, L., Parks, T. L., Schneider, D. K., Kiser, R. F., Coalter, V. J., Walsh, G. & other authors (2000). Containment of simian immunodeficiency virus infection: cellular immune responses and protection from rechallenge following transient postinoculation antiretroviral treatment. *J Virol* **74**, 2584–2593.

Liu, J., Wang, S., Hoxie, J. A., LaBranche, C. C. & Lu, M. (2002). Mutations that destabilize the gp41 core are determinants for stabilizing the simian immunodeficiency virus-CPmac envelope glycoprotein complex. *J Biol Chem* **277**, 12891–12900.

Maerz, A. L., Drummer, H. E., Wilson, K. A. & Poumbourios, P. (2001). Functional analysis of the disulfide-bonded loop/chain reversal region of human immunodeficiency virus type 1 gp41 reveals a critical role in gp120-gp41 association. *J Virol* **75**, 6635–6644.

Means, R. E., Greenough, T. & Desrosiers, R. C. (1997). Neutralization sensitivity of cell culture-passaged simian immunodeficiency virus. *J Virol* **71**, 7895–7902.

Miyazawa, M., Nishio, J., Wehrly, K. & Chesebro, B. (1992). Influence of MHC genes on spontaneous recovery from Friend retrovirus-induced leukemia. *J Immunol* **148**, 644–647.

Mori, K., Yasutomi, Y., Sawada, S., Villinger, F., Sugama, K., Rosenwith, B., Heeney, J. L., Uberla, K., Yamazaki, S. & other authors (2000). Suppression of acute viremia by short-term postexposure prophylaxis of simian/human immunodeficiency virus SHIV-RT-infected monkeys with a novel reverse transcriptase inhibitor (GW420867) allows for development of potent antiviral immune responses resulting in efficient containment of infection. *J Virol* **74**, 5747–5753.

Mori, K., Yasutomi, Y., Ohgimoto, S., Nakasone, T., Takamura, S., Shioda, T. & Nagai, Y. (2001). Quintuple deglycosylation mutant of simian immunodeficiency virus SIVmac239 in rhesus macaques: robust primary replication, tightly contained chronic infection, and elicitation of potent immunity against the parental wild-type strain. *J Virol* **75**, 4023–4028.

Mori, K., Sugimoto, C., Ohgimoto, S., Nakayama, E. E., Shioda, T., Kusagawa, S., Takebe, Y., Kano, M., Matano, T. & other authors (2005). Influence of glycosylation on the efficacy of an Env-based vaccine against simian immunodeficiency virus SIVmac239 in a macaque AIDS model. *J Virol* **79**, 10386–10396.

Muster, T., Steindl, F., Purtscher, M., Trkola, A., Klima, A., Himmler, G., Ruker, F. & Katinger, H. (1993). A conserved neutralizing epitope on gp41 of human immunodeficiency virus type 1. *J Virol* **67**, 6642–6647.

Nishimura, Y., Igarashi, T., Haigwood, N., Sadjadpour, R., Plishka, R. J., Buckler-White, A., Shibata, R. & Martin, M. A. (2002). Determination of a statistically valid neutralization titer in plasma that confers protection against simian-human immunodeficiency virus challenge following passive transfer of high-titered neutralizing antibodies. *J Virol* **76**, 2123–2130.

Nyambi, P. N., Gorny, M. K., Bastiani, L., van der Groen, G., Williams, C. & Zolla-Pazner, S. (1998). Mapping of epitopes exposed on intact human immunodeficiency virus type 1 (HIV-1) virions: a new strategy for studying the immunologic relatedness of HIV-1. *J Virol* **72**, 9384–9391.

O'Connor, D. H., Mothe, B. R., Weinfurter, J. T., Fuenger, S., Rehrauer, W. M., Jing, P., Rudersdorf, R. R., Liebl, M. E., Krebs, K. & other authors (2003). Major histocompatibility complex class I alleles associated with slow simian immunodeficiency virus disease progression bind epitopes recognized by dominant acute-phase cytotoxic-T-lymphocyte responses. *J Virol* **77**, 9029–9040.

Ohgimoto, S., Shioda, T., Mori, K., Nakayama, E. E., Hu, H. & Nagai, Y. (1998). Location-specific, unequal contribution of the *N* glycans in simian immunodeficiency virus gp120 to viral infectivity and removal of multiple glycans without disturbing infectivity. *J Virol* **72**, 8365–8370.

Pinschewer, D. D., Perez, M., Jeetendra, E., Bachi, T., Horvath, E., Hengartner, H., Whitt, M. A., de la Torre, J. C. & Zinkernagel, R. M. (2004). Kinetics of protective antibodies are determined by the viral surface antigen. *J Clin Invest* **114**, 988–993.

Puffer, B. A., Pohlmann, S., Edinger, A. L., Carlin, D., Sanchez, M. D., Reitter, J., Watry, D. D., Fox, H. S., Desrosiers, R. C. & Doms, R. W. (2002). CD4 independence of simian immunodeficiency virus Envs is associated with macrophage tropism, neutralization sensitivity, and attenuated pathogenicity. *J Virol* **76**, 2595–2605.

Regier, D. A. & Desrosiers, R. C. (1990). The complete nucleotide sequence of a pathogenic molecular clone of simian immunodeficiency virus. *AIDS Res Hum Retroviruses* **6**, 1221–1231.

Reimann, K. A., Parker, R. A., Seaman, M. S., Beaudry, K., Beddall, M., Peterson, L., Williams, K. C., Veazey, R. S., Montefiori, D. C. & other authors (2005). Pathogenicity of simian-human immunodeficiency virus SHIV-89.6P and SIVmac is attenuated in cynomolgus macaques and associated with early T-lymphocyte responses. *J Virol* **79**, 8878–8885.

Reitter, J. N., Means, R. E. & Desrosiers, R. C. (1998). A role for carbohydrates in immune evasion in AIDS. *Nat Med* **4**, 679–684.

Schmitz, J. E., Johnson, R. P., McClure, H. M., Manson, K. H., Wyand, M. S., Kuroda, M. J., Lifton, M. A., Khunkhun, R. S., McEvers, K. J. & other authors (2005). Effect of $CD8^+$ lymphocyte depletion on virus containment after simian immunodeficiency virus SIVmac251 challenge of live attenuated SIVmac239Δ3-vaccinated rhesus macaques. *J Virol* **79**, 8131–8141.

Silvera, P., Flanagan, B., Kent, K., Rud, E., Powell, C., Corcoran, T., Bruck, C., Thiriart, C., Haigwood, N. L. & Stott, E. J. (1994). Fine analysis of humoral antibody response to envelope glycoprotein of SIV in infected and vaccinated macaques. *AIDS Res Hum Retroviruses* **10**, 1295–1304.

Smith, D. G. & McDonough, J. (2005). Mitochondrial DNA variation in Chinese and Indian rhesus macaques (*Macaca mulatta*). *Am J Primatol* **65**, 1–25.

Wei, X., Decker, J. M., Wang, S., Hui, H., Kappes, J. C., Wu, X., Salazar-Gonzalez, J. F., Salazar, M. G., Kilby, J. M. & other authors (2003). Antibody neutralization and escape by HIV-1. *Nature* **422**, 307–312.

Wyatt, R. & Sodroski, J. (1998). The HIV-1 envelope glycoproteins: fusogens, antigens, and immunogens. *Science* **280**, 1884–1888.

Wyatt, R., Kwong, P. D., Desjardins, E., Sweet, R. W., Robinson, J., Hendrickson, W. A. & Sodroski, J. G. (1998). The antigenic structure of the HIV gp120 envelope glycoprotein. *Nature* **393**, 705–711.

York, J. & Nunberg, J. H. (2004). Role of hydrophobic residues in the central ectodomain of gp41 in maintaining the association between human immunodeficiency virus type 1 envelope glycoprotein subunits gp120 and gp41. *J Virol* **78**, 4921–4926.

Yu, D., Shioda, T., Kato, A., Hasan, M. K., Sakai, Y. & Nagai, Y. (1997). Sendai virus-based expression of HIV-1 gp120: reinforcement by the V(−) version. *Genes Cells* **2**, 457–466.

Zhang, M., Gaschen, B., Blay, W., Foley, B., Haigwood, N., Kuiken, C. & Korber, B. (2004). Tracking global patterns of *N*-linked glycosylation site variation in highly variable viral glycoproteins: HIV, SIV, and HCV envelopes and influenza hemagglutinin. *Glycobiology* **14**, 1229–1246.

Zolla-Pazner, S. (2004). Identifying epitopes of HIV-1 that induce protective antibodies. *Nat Rev Immunol* **4**, 199–210.

Journal of Medical Virology 80:373–382 (2008)

Comparison Between Sendai Virus and Adenovirus Vectors to Transduce HIV-1 Genes Into Human Dendritic Cells

Noriaki Hosoya,[1] Toshiyuki Miura,[1] Ai Kawana-Tachikawa,[1] Tomohiko Koibuchi,[1] Tatsuo Shioda,[2] Takashi Odawara,[3] Tetsuya Nakamura,[3] Yoshihiro Kitamura,[1] Munehide Kano,[4] Atsushi Kato,[5] Mamoru Hasegawa,[6] Yoshiyuki Nagai,[7] and Aikichi Iwamoto[1,3,8,9,10]*

[1]*Division of Infectious Diseases, Advanced Clinical Research Center, The Institute of Medical Science, The University of Tokyo, Minato-ku, Tokyo, Japan*
[2]*Department of Viral Infections, Research Institute of Microbial Diseases, Osaka University, Osaka, Japan*
[3]*Department of Infectious Diseases and Applied Immunology, Research Hospital, The Institute of Medical Science, The University of Tokyo, Tokyo, Japan*
[4]*AIDS Research Center, National Institute of Infectious Diseases, Tokyo, Japan*
[5]*Department of Virology 3, National Institute of Infectious Diseases, Tokyo, Japan*
[6]*DNAVEC Research, Inc., Ibaraki, Japan*
[7]*Center of Research Network for Infectious Diseases, Riken, Tokyo, Japan*
[8]*International Research Center for Infectious Diseases, The Institute of Medical Science, The University of Tokyo, Tokyo, Japan*
[9]*Japan-China Joint Laboratory of Structural Virology and Immunology, Institute of Biophysics, Chinese Academy of Sciences, Beijing, China*
[10]*Japan-China Joint Laboratory of Molecular Immunology and Molecular Microbiology, Institute of Microbiology, Chinese Academy of Sciences, Beijing, China*

Immuno-genetherapy using dendritic cells (DCs) can be applied to human immunodeficiency virus type 1 (HIV-1) infection. Sendai virus (SeV) has unique features such as cytoplasmic replication and high protein expression as a vector for genetic manipulation. In this study, we compared the efficiency of inducing green fluorescent protein (GFP) and HIV-1 gene expression in human monocyte-derived DCs between SeV and adenovirus (AdV). Human monocyte-derived DCs infected with SeV showed the maximum gene expression 24 hr after infection at a multiplicity of infection (MOI) of 2. Although SeV vector showed higher cytopathic effect on DCs than AdV, SeV vector induced maximum gene expression earlier and at much lower MOI. In terms of cell surface phenotype, both SeV and AdV vectors induced DC maturation. DCs infected with SeV as well as AdV elicited HIV-1 specific T-cell responses detected by interferon γ (IFN-γ) enzyme-linked immunospot (Elispot). Our data suggest that SeV could be one of the reliable vectors for immuno-genetherapy for HIV-1 infected patients. ***J. Med. Virol. 80:373–382, 2008.*** © 2008 Wiley-Liss, Inc.

KEY WORDS: viral vector; immuno-genetherapy; AIDS

INTRODUCTION

Introduction of highly active anti-retroviral therapy (HAART) has improved the clinical course of patients infected with human immunodeficiency virus type 1 (HIV-1) dramatically. However, there are many obstacles to the long-term administration of anti-retroviral drugs, such as metabolic disorders, emergence of drug resistant viruses, and high medical expenses. The combination of therapeutic vaccines and HAART could not only reduce the adverse effects of HAART but also decrease the medical expenses especially in developing countries.

Cellular immune responses play a crucial role in controlling the replication of HIV-1 [Yang et al., 1997;

Grant sponsor: AIDS Research from the Ministry of Health, Labor and Welfare of Japan (partial support); Grant sponsor: Special Coordination Funds for Promoting Science and Technology of MEXT: Strategic cooperation to control emerging and reemerging infections.

*Correspondence to: Aikichi Iwamoto, Division of Infectious Diseases, Advanced Clinical Research Center, The Institute of Medical Science, The University of Tokyo, 4-6-1 Shirokanedai, Minato-ku, Tokyo 108-8639, Japan.
E-mail: aikichi@ims.u-tokyo.ac.jp

Accepted 5 September 2007
DOI 10.1002/jmv.21052
Published online in Wiley InterScience (www.interscience.wiley.com)

Matano et al., 1998; Brander and Walker, 1999; Jin et al., 1999; McMichael and Rowland-Jones, 2001]. One of the possible strategies for treating HIV-1 infection is to enhance the cellular anti-viral capacity. Since dendritic cells (DCs) have high ability of antigen presentation, they have been used as stimulators of T-cell responses by inserting HIV-1 antigens [Engelmayer et al., 2001; Stubbs et al., 2001; Tsunetsugu-Yokota et al., 2003; Mwau et al., 2004].

Sendai virus (SeV), one of the members of *Paramyxoviridae*, is an enveloped virus with a nonsegmented negative-strand RNA genome. It causes severe respiratory disease in mice but is nonpathogenic for humans. SeV vector has been developed and shown to have high gene transduction efficiency and protein expression in different cell lineages [Kato et al., 1996; Kawana-Tachikawa et al., 2002]. In addition, the cytoplasmic replication of SeV precludes the integration of its genetic information into cellular genome. Recently, the second generation SeV vector deficient in F gene (dF-SeV) has been developed [Li et al., 2000]. The dF-SeV has been proved not to cause secondary infection. SeV and dF-SeV vectors could be promising systems to introduce HIV-1 genes into DCs for stimulating HIV-1 specific T-cell responses in primates and humans [Kano et al., 2002; Takeda et al., 2003; Kato et al., 2005].

Adenovirus (AdV), vaccinia virus, and retrovirus have been used as viral vectors for gene transfer into DCs [Engelmayer et al., 1999; Rea et al., 1999; Bonini et al., 2001; Rouas et al., 2002]. In this study, we compared the efficiency of inducing green fluorescent protein (GFP) and HIV-1 gene expression in human monocyte-derived DCs between AdV vectors and new viral vectors based on SeV. We showed that SeV vector transduced DCs efficiently and elicited HIV-1 specific T-cell responses. Our results suggest the potential use of SeV vector for immuno-genetherapy for HIV-1 infected patients.

MATERIALS AND METHODS

Viral Vectors

SeV carrying GFP (SeVGFP) [Agungpriyono et al., 2000], HIV-1 NL4-3 Gag (SeVGag), and HIV-1 SF2 Env (SeVEnv) [Yu et al., 1997] were propagated in 10-day-old embryonated chicken eggs. The fusion protein (F)-defective SeV (dF-SeV) [Li et al., 2000] was propagated in the monkey kidney cell line expressing Sendai virus F gene product (LLC-MK2/F7) [Li et al., 2000] because the replication capacity of dF-SeV was incompetent. SeV particles were purified by 50% sucrose (w/v)/10 mM Tris–HCl and 30% sucrose (w/v)/10 mM Tris–HCl density centrifugation, dialyzed against Dulbecco's phosphate buffered saline (PBS) (Sigma, St. Louis, MO), and stored at −80°C. The titers of the vector stocks, determined on LLC-MK2 [Kato et al., 1996], were as follows; SeVGag: 5.2×10^8 CIU/ml, SeVEnv: 6.4×10^7 CIU/ml, SeVGFP: 5.2×10^8 CIU/ml, GFP/dF-SeV: 3.1×10^9 CIU/ml, SeV without inserts: 5.2×10^8 CIU/ml.

Recombinant AdV used in this experiment was derived from AdV type 5 and was replication-deficient with deletion of E1 and E3 genes. The AdV carrying HIV-1 genes (*gag-pol*, *env*, *rev*, and RRE) was generated with AdV Expression Kit (TakaraBio, Shiga, Japan) according to the manufacturer's protocol. Each HIV-1 gene was inserted into the expression cassette of pAxCAwt cosmid vector equipped with CAG promoter and rabbit beta-globin polyadenylation signal. All HIV-1 sequences were derived from SF2 strain [Levy et al., 1986]. 5′ half and 3′ half of *Eco*RI fragments from SF2 provirus were subcloned pUC19, generating pUC19-9B/R7 and pUC19-9B/R6, respectively. HIV-1 *gag-pol* gene was obtained from pUC19-9B/R7 after deleting the sequence upstream of *gag*. *Nar*I site was introduced next to gag initiation codon by PCR using primers *gag*/*Nar*I-S (5′-CAGGCGGCAAGGAGAGAGATGGGTGC-GAG-3′) and *gag*/*Apa*I-AS (5′-CCTTTTTCCTAGGGG-CCCTGC-3′) (restriction sites are underlined). PCR-amplified fragment was returned to *Nar*I and *Apa* I-digested pUC19-9B/R7, generating pUC19-GP. The 4.5 kb *Nar*I-*Nde*I fragment containing the HIV-1 *gag-pol* gene was inserted into the *Swa*I site of pAxCAwt cosmid vector to create AdVGP. HIV-1 *rev* responsible element (RRE) was generated from pUC19-9B/R6 by PCR using primers rre/*pfl*MI-S (5′-GCCATAGAATG-GCCAAGGCAAAGAGAAGAGTGG-3′) and rre/*Bam*HI-AS (5′-GGGATCCCAAGGCACAGCAGTGGTTGC-3′). The PCR fragment was inserted between *pfl*MI and *Bam*HI site of pUC19-GP, and thus placed downstream of *gag-pol* gene. The consequent 4.9 kb *Nar*I-*Bam*HI fragment containing the HIV-1 *gag-pol*-RRE sequences was inserted into the *Swa*I site of pAxCAwt cosmid vector to create AdVGPR. HIV-1 *rev* gene was made by two-step PCR from *Stu*I-*Xho*I fragment of pUC19-9B/R6. The 1st-PCR primer set was *rev*/1st-S (5′-CTCA-GGACAGTCAGACTCATCAAGCTTCTCTATCAAAG-CAACCCGCCTCC-3′) and *rev*-AS (5′-GGCTATTCTT-TAGTTCCTGAATCCAATACTGCA-3′), and the 2nd-PCR primer set was *rev*/2nd-S (5′-GGATGGCAGGAA-GAAGCGGAGACAGCGACGAAGAGCTCCTCAGGA-CAG-3′) and *rev*-AS. The PCR fragment was digested with *Sph*I and *Spe*I, and inserted into the *Swa*I site of pAxCAwt to create AdVRev. The absence of PCR errors was confirmed for all PCR-amplified fragments by sequencing. The 2.1 kb *Mlu*I-*Xho*I fragment of pUC19-9B/R6 containing the HIV-1 *env* gene was inserted into the *Swa*I site of pAxCAwt cosmid vector to create AdVEnv. Recombinant AdV, Ax1w1 [Miyake et al., 1996] bearing no insert and AdVGFP [Miyake et al., 1996] expressing GFP, were kindly provided by Dr. Izumu Saito and Yumi Kanegae (University of Tokyo, Tokyo, Japan). AdV was propagated in 293 cells [Graham et al., 1977], purified by two rounds of CsCl density centrifugation [Kanegae et al., 1994], dialyzed against PBS containing 10% glycerol and stored at −80°C. The titer of the viral stocks was determined by a plaque-forming assay on 293 cells. The titers of each virus were as follows; AdVGPR: 7.6×10^9 pfu/ml, AdVEnv: 1.6×10^{11} pfu/ml, AdVRev: 2.7×10^{11} pfu/ml, AdVGFP: 5.9×10^{10} pfu/ml, Ax1w1: 4.7×10^{11} pfu/ml. Vector stocks were tested for the

absence of replication-competent AdV as described [Ishii-Watabe et al., 2003].

Cell Lines and Media

Monkey kidney cell line (LLC-MK2) was cultured in minimal essential medium (MEM) (Sigma) supplemented with 100 U of penicillin/ml, 100 U of streptomycin/ml, and 10% heat-inactivated fetal calf serum (FCS). Two hundred ninety three cells were cultured in Dulbecco's modified eagle medium (DMEM) (Sigma) supplemented with 100 U of penicillin/ml, 100 U of streptomycin/ml, and 10% FCS.

Generation of DCs

Immature myeloid DCs were generated from human peripheral blood mononuclear cells (PBMCs) using previously described methods [Nagayama et al., 2003]. Briefly, PBMCs of healthy adult volunteers were collected in heparinized tubes, subjected to density centrifugation over Ficoll-Paque Plus (Amersham Pharmacia Biotech, Piscataway, NJ), and washed twice with PBS. These PBMCs were plated on 10 cm PRIMARIA tissue culture dish (Becton Dickinson Labware, FranklinLakes, NJ) and kept at 37°C for 30 min to remove nonadherent cells. Floating cells were removed gently by rinsing with 10 ml of PBS three times and the remaining adherent cells were cultured overnight in 6 ml of RPMI 1640 medium at 37°C. Cells were washed three times again on the next day with 10 ml of PBS and the remaining adherent cells were cultured for 7 days in DC medium [6 ml of RPMI 1640 supplemented with 100 U of penicillin/ml, 10 mg of streptomycin/ml, and 10% FCS, 300 ng of recombinant human granulocyte-macrophage colony stimulating factor (rhGM-CSF) (Wako, Osaka, Japan), and 300 ng of recombinant human interleukin-4 (rhIL-4) (Wako)]. After 7 days, DCs were collected with a scraper. Tumor necrosis factor-α (TNF-α) (Wako) was added to the DC medium at a final concentration of 50 ng/ml on day 7 in some experiments and cultured for another 2 days to generate mature DCs. The purity of DCs was >95% based on the expression of CD1a and CD11c and lack of expression of T-cell, B-cell, NK-cell, and monocyte lineage markers by flow cytometry (data not shown).

Infection of DCs With Viral Vectors

5×10^5 DCs were infected with SeV or AdV vectors for 1 hr at 37°C in a final volume of at least 500 μl of serum-free RPMI 1640. After the infection, DCs were washed with serum-free RPMI 1640 medium and cultured in 24 well plates with 1 ml of the DC medium.

SDS-PAGE and Western Blot Analysis

DCs infected with SeV (SeVGag or SeVEnv) at a multiplicity of infection (MOI) of 2 or with AdV (AdVGFR, AdVEnv, AdVRev) at an MOI of 1,000 were harvested after 24 or 48 hr of infection, respectively. After washing with PBS, the cells were resuspended in RIPA buffer (10 mM Tris–HCl [pH 7.4], 150 mM NaCl, 1% NP-40, 0.1% sodium deoxycholate, 0.1% sodium dodecyl sulfate (SDS), 1 mM EDTA, complete mini as 1× protease inhibitor cocktail [Roche, Basel, Switzerland]), and kept on ice for 10 min. The suspension was spun for 5 min at 9,000*g* to remove cell debris. The amount of protein in the cell lysate was determined by protein assay kit (Bio-Rad Laboratories, Hercules, CA). Cell lysates containing 30 μg of cellular protein were loaded onto a 10–20% Ready Gels J (Bio-Rad Laboratories) and electrophoretically transferred to immobilon polyvinylidene difluoride transfer membrane (Millipore, Billerica, MA). Western blot analysis was performed using Lumi-Light plus Western Blotting Kit (Roche) according to the manufacturer's instructions. Briefly, the membrane was blocked in 1% blocking solution at 4°C overnight. The membrane was incubated with mouse monoclonal antibodies against p24 (Advanced Biotechnologies, Inc., Columbia, MD) and gp120 (Immuno Diagnostics, Inc., Woburn, MA) of HIV-1 for 1 hr. The blots were then washed four times with 1× TBST and incubated with anti-mouse IgG conjugated with horseradish peroxidase (Roche). Proteins were illuminated by Lumilight Plus (Roche) and detected with Lumi Imager (Roche). Quantification was done by densitometric analysis with the Lumi Analyst software (Roche).

Immunostaining and Flow Cytometry

GFP expression and viability of DCs infected with SeVGFP, dF-SeVGFP, or AdVGFP were analyzed by flow cytometry. To determine the viability, 5×10^5 DCs in about 300 μl of media were stained with 10 μl of propidium iodide (PI) (50 μg/ml; SIGMA). Events were acquired on a FACS-Caliber (Becton Dickinson) and analyzed with CellQuest software (Becton Dickinson) and Flow Jo software version 4.1 (Tree Star, Asland, OK).

To determine the effects of transduction on the expression of DC surface marker, immature DCs (imDCs) were cultured with the DC medium for 48 hr, mature DCs (mDCs) were cultured with the DC medium plus TNF-α for 48 hr. DCs transduced with SeV or AdV were cultured with the DC medium for 24 or 48 hr, respectively. Those DCs were stained with antibodies at 4°C for 20 min and then washed three times with PBS. Those cells were analyzed by flow cytometry after fixing 1% paraformaldehyde. The antibodies we used were as follows: fluorescein isothiocyanate-anti-Lineage (Lin-FITC) (CD3, CD14, CD16, CD19, CD20, CD56) (Becton Dickinson), phycoerythrin (PE)-anti-CD1a (Immunotech, Marseilles, France), PE-anti-CD83 (Immunotech), PE-anti-HLA-ABC (Dako), Peridinin chlorophyll protein (PerCP) -anti-CD4 (Becton Dickinson), PerCP-anti-HLA-DR (Becton Dickinson), allophycocyanin (APC)-anti-CD14 (Immunotech), APC-anti-CD40 (PharMingen), APC-anti-CD11c (PharMingen), Biotin-conjugated anti-CD86 (Becton Dickinson). Streptavidin-FITC (Becton